



# **Grain-scale measurements of particle-fluid interaction in marine and aeolian sediment transport**

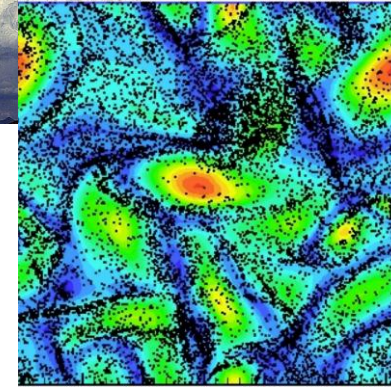
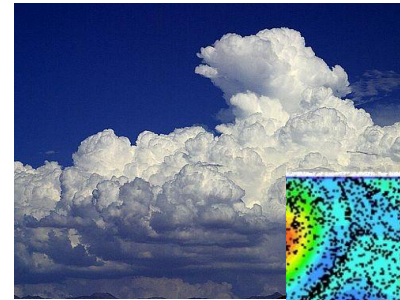
**Ken Kiger**  
**Department of Mechanical Engineering**  
**University of Maryland**

**KITP Workshop: Fluid Mediated Particle Transport in Geophysical Flows**  
**October 3, 2013**

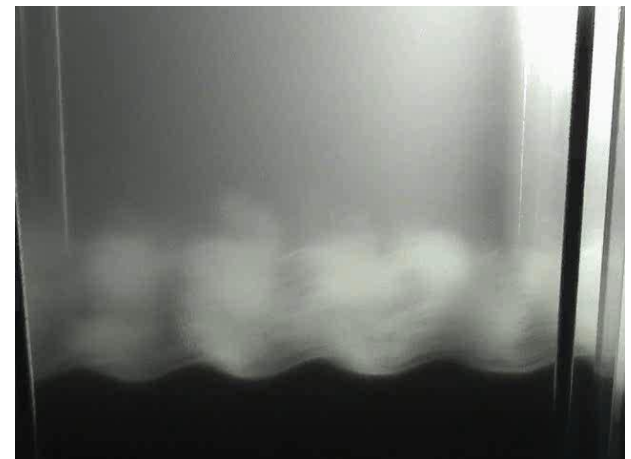
**Work supported by the NSF and AFSOR**

# Measurement of dispersed two-phase flows

- **Physics of collective fluid/particle coupling poorly understood**
  - What are the effective sediment turbulence characteristics?
  - Is purely stochastic description adequate?
  - How do anisotropic flow structures influence net coupling?
- **Primary variables of interest:**
  - Velocity of suspending fluid
  - Velocity of particulates (sediment)
  - Concentration of particulates
  - Size distribution
- **Goals**
  - Simultaneous measurement of fluid and dispersed phase motion
    - *Quantify fluid motion responsible for turbulent suspension of particles*
    - *Quantify nature of flow modification and particle/turbulence interaction*

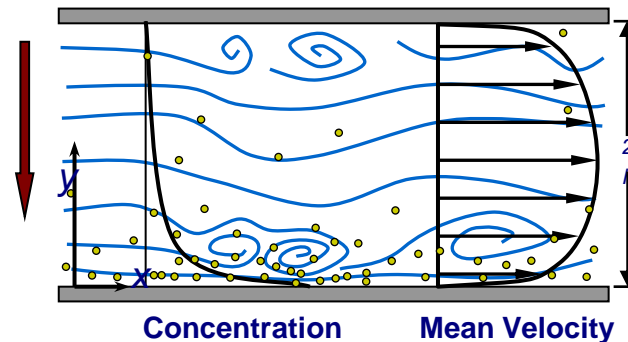


M. Garcia,  
[http://www.cerfacs.fr/cfd/FIGURES/IMAGES/vort\\_stokes2-MG.jpg](http://www.cerfacs.fr/cfd/FIGURES/IMAGES/vort_stokes2-MG.jpg)



# Overview

- **Two-fluid framework and closure**
- **Experimental techniques**
- **Prototypical flow: fully developed channel flow**
  - Solid-liquid suspension



- **Complex applied flow: rotorcraft downwash**
  - Solid-gas suspension



# Problem Framework: Two-Fluid Equations

- **Apply averaging operator to mass and momentum equations**

- Drew (1983), Simonin (1991)

- *Phase indicator function*

$$\chi_k(x_i, t) = \begin{cases} 1 & \text{if } x_i \text{ inside phase } k \\ 0 & \text{if } x_i \text{ outside phase } k \end{cases} \quad \frac{\partial \chi_k}{\partial t} + u_{I,j} \frac{\partial \chi_k}{\partial x_j} = 0$$

- *Averaging operator*

$$\alpha_k = \langle \chi_k \rangle, \text{ volume fraction} \quad \alpha_k G_{k,ij} = \langle \chi_k g_{ij} \rangle \quad g'_{ij} = g_{ij} - G_{2,ij}$$

- Assume no inter-phase mass flux, incompressible carrier phase

- *Mass*

$$\frac{\partial}{\partial t} (a_k r_k) + \frac{\partial}{\partial x_j} (a_k r_k U_{k,j}) = 0$$

$\tau_{k,ij}$  = averaged viscous stress tensor in phase  $k$

- *Momentum*

$I_{k,i}$  = Mean interphase momentum transport  
(less mean pressure contribution)

$$a_k r_k \frac{\partial U_{k,i}}{\partial t} + U_{k,j} \frac{\partial}{\partial x_j} (a_k r_k U_{k,i}) = -a_k \frac{\partial P_1}{\partial x_i} + a_k r_k g_i + \frac{\partial}{\partial x_j} (a_k t_{k,ij}) - \frac{\partial}{\partial x_j} (a_k r_k \langle u_i u_j \rangle_k) + I_{k,i}$$



# Two-Fluid Equations (cont)

- **Interphase momentum transport**
  - Dilute flow: no particle-particle interactions
  - For large particle/fluid density ratios, quasi-steady viscous drag is by far the dominant term
    - *For small density ratios, additional force terms can be relevant*
      - Added mass, Pressure term, Basset history term etc.
  - For sediment,  $\rho_2/\rho_1 \sim 2.5 > 1$  ( $k=1$  for fluid,  $k=2$  for dispersed phase)
    - *Drag still first order effect, but other terms will likely also contribute*

$$I_{2,i} = -I_{1,i} = -\alpha_k \left\langle \rho_1 \frac{3}{4} \frac{C_D}{d} |\mathbf{v}_r| \mathbf{v}_{r,i} \right\rangle_2$$

$$\mathbf{v}_{r,i} = \mathbf{u}_{2,i} - \mathbf{u}_{1,i} \quad C_D = \frac{24 \left[ 1 + 0.15 \text{Re}_p^{0.687} \right]}{\text{Re}_p} \quad \text{Re}_p = \frac{\rho_1 |\mathbf{v}_r| d}{\mu_1}$$

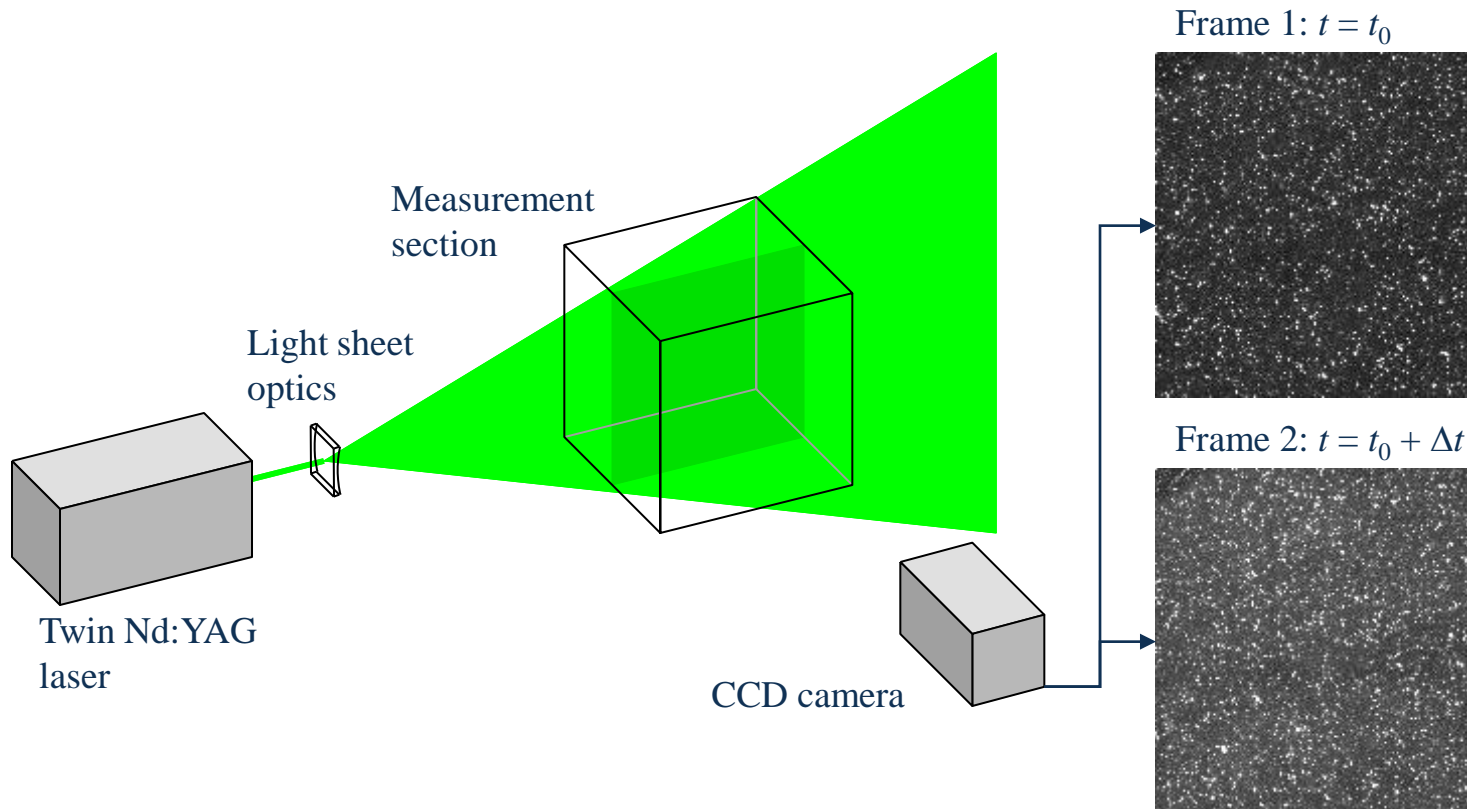
# Closure requirements

- **Closure is needed for:**
  - *Particle fluctuations*
  - *Particle/fluid cross-correlations*
  - *Fluid fluctuations*
- Simplest method is to use a gradient transport (mixing length) model
  - *Shown to be inconsistent for many applications*
- Alternative: Provide separate evolution equation for higher order terms
  - Particle kinetic stress equation
  - Particle/fluid covariance equation
  - Fluid kinetic stress equation
  - *Will require third-moment correlations models to complete the closure*
- **Experiments**
  - Simultaneous measurements of both fluid and particles are needed
    - *Provides check for model developments*
    - *Can be performed under conditions not readily accessible to DNS/LES*
      - Particles larger than the turbulent fluid scales, finite  $Re_p$

# What is PIV? (single phase flow)

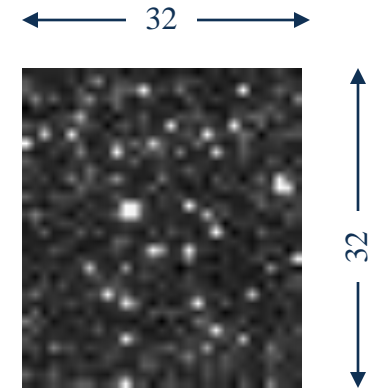
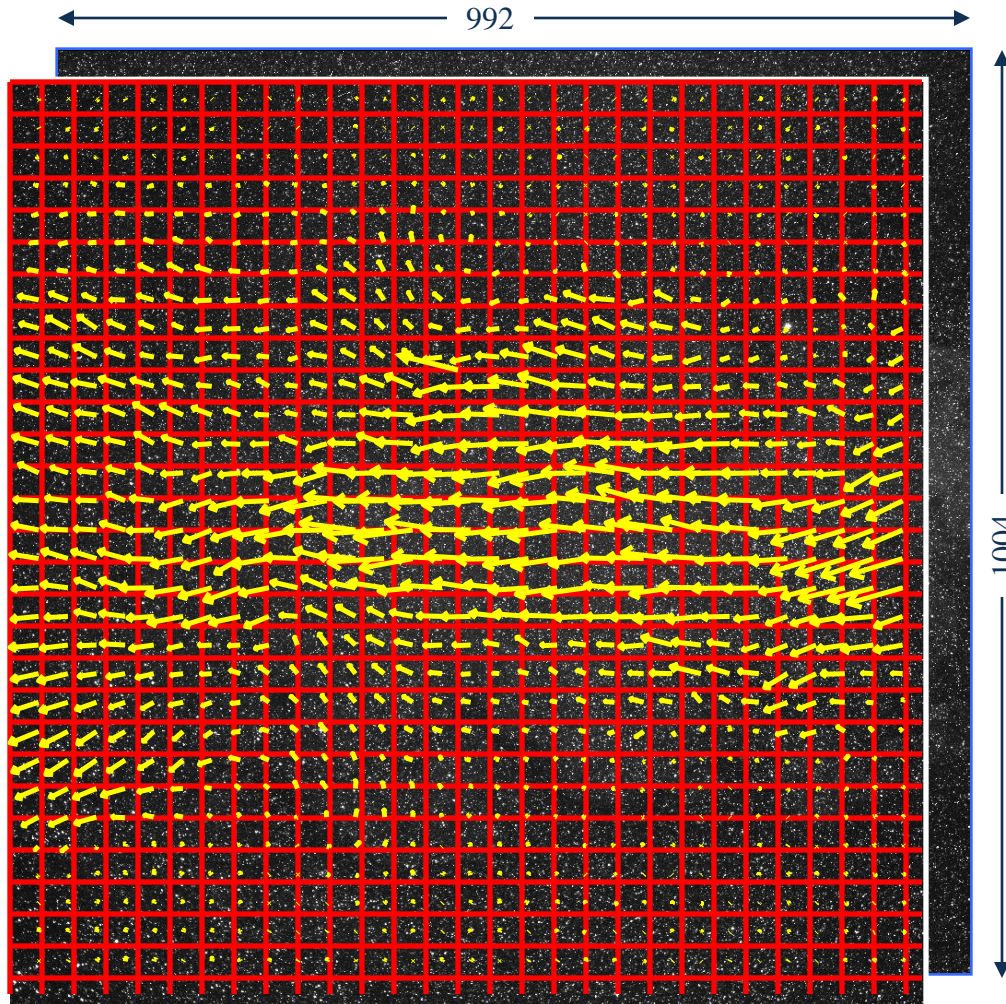
Particle Image Velocimetry (PIV):

Quantitative imaging method to infer local fluid motion from displacement of tracer particles



# Result of PIV interrogation

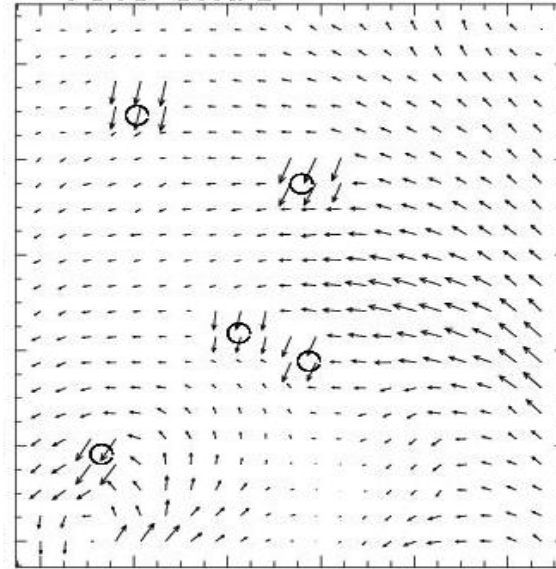
Particle Image Velocimetry (PIV)



- divide image pair in *interrogation regions*
- small region:  
~ uniform motion
- compute displacement
- *repeat !!!*

# Difficulty with Two-Phase PIV

- **Coupled but distinct motion in different phases**

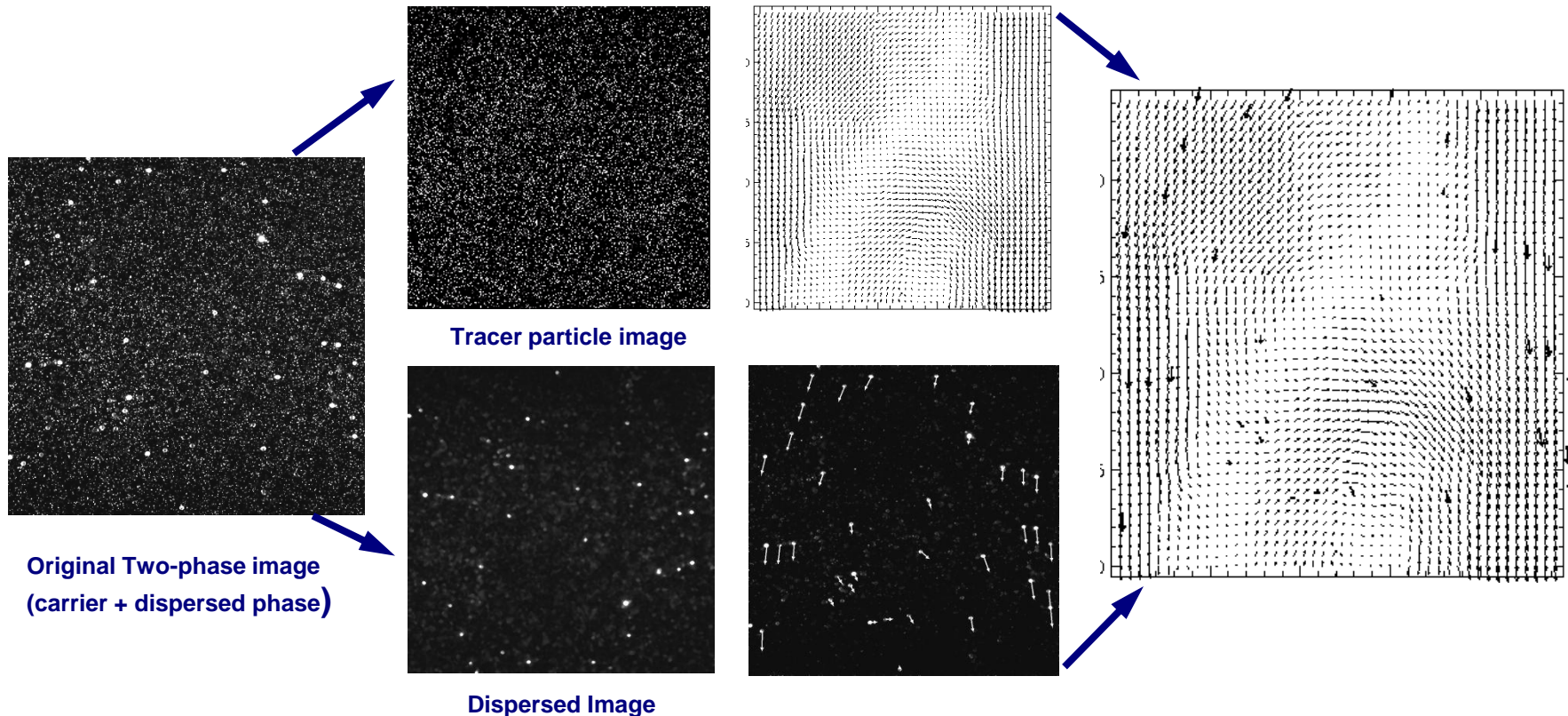


- **Need to separate the images of the phases**
  - How to discriminate the sediment from the fluid? *Image characteristics*
- **Strengths**
  - Snapshot of flow structure (fluid velocity, sediment velocity, concentration)
- **Limitations**
  - Flow must be optically dilute (must see through it, volume fraction  $< 1\%$ )
  - Usually prefer large size separation between tracer seed and dispersed phase
  - Difficult to reliably discriminate size
  - Dynamic range: 100 to 1 is typical, can be better, but challenging



# Single camera Two-Phase PIV Implementation

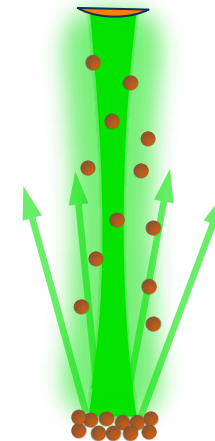
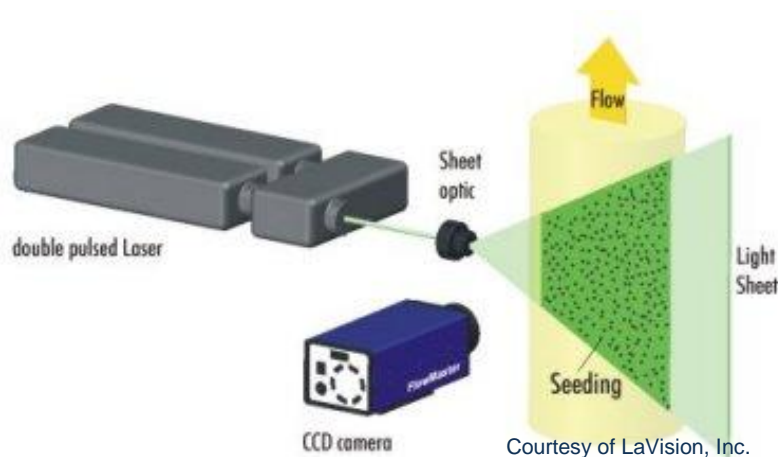
- **Simultaneous Velocity Measurement of both phases**
  - *Use median filtering technique to separate images*
  - *Particle tracking of dispersed phase*
    - combine with size/intensity filter (Khalitov & Longmire, 2002)
  - *Cross-correlation PIV of carrier fluid*



# Dispersed phase measurement by sheet illumination

- **Sheet illumination considerations**

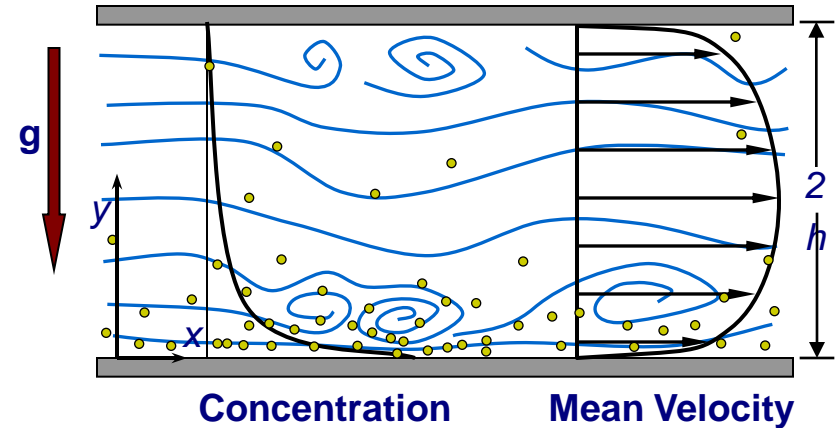
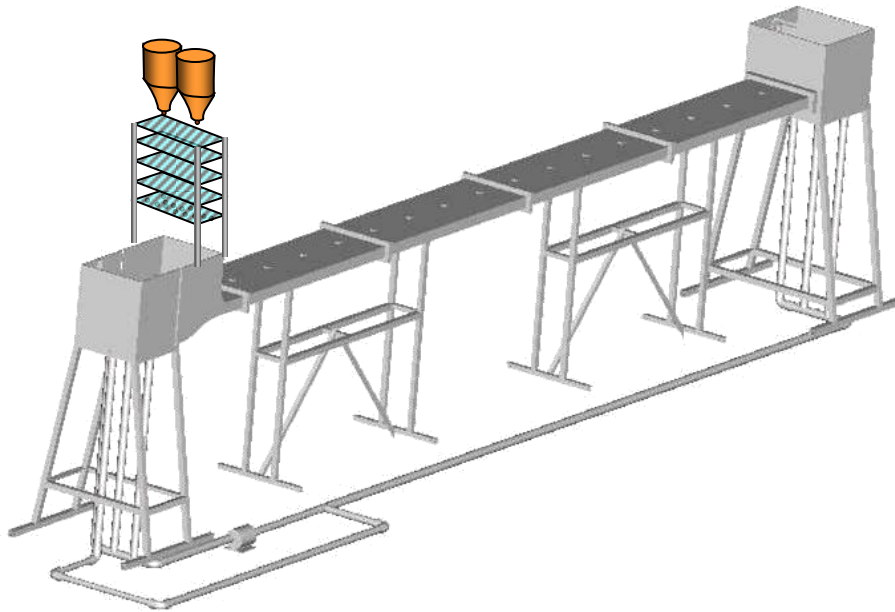
- What is the effective sampling volume for a particle in a light sheet? Can't we just count particles?



- **Works fine for small image regions far from boundaries, but in general one needs to account for:**

- Focusing & attenuation of sheet
- Scattered illumination
- Boundary reflections

# Experimental Facility



- **Planar Horizontal Water Channel**
  - $4 \times 36 \times 488$  cm, recirculating flow
  - Pressure gradient measurements
    - *fully-developed by  $x = 250$  cm*
  - Particles introduced to settling chamber outlet across span

# Experimental Conditions

- **Both single-phase and two-phase experiments conducted**
- **Carrier Fluid Conditions**
  - Water,  $Q = 7.6$  l/s
  - $U_c = 59$  cm/s,  $u_\tau = 2.8$  cm/s,  $Re_\tau = 570$
  - Flowrate kept the same for two-phase experiments
  - Tracer particles:  $10\ \mu\text{m}$  silver-coated, hollow glass spheres,  $SG = 1.4$
- **Dispersed Phase Conditions**
  - Glass beads: (specific gravity,  $SG = 2.5$ )
  - Standard sieve size range:  $180 < D < 212\ \mu\text{m}$
  - Settling velocity,  $v_s = 2.2$  to  $2.6$  cm/s
  - Corrected Particle Response Time,  $\tau_p = 4.5$  ms
  - $St^+ = \tau_p/\tau^+ \sim 4$
  - Bulk Mass Loading:  $dM/dt = 4$  gm/s,  $M_p/M_f \sim 5 \times 10^{-4}$
  - Bulk Volume Fraction,  $\alpha = 2 \times 10^{-4}$

# Two-Phase Flow: Mean Concentration Profile

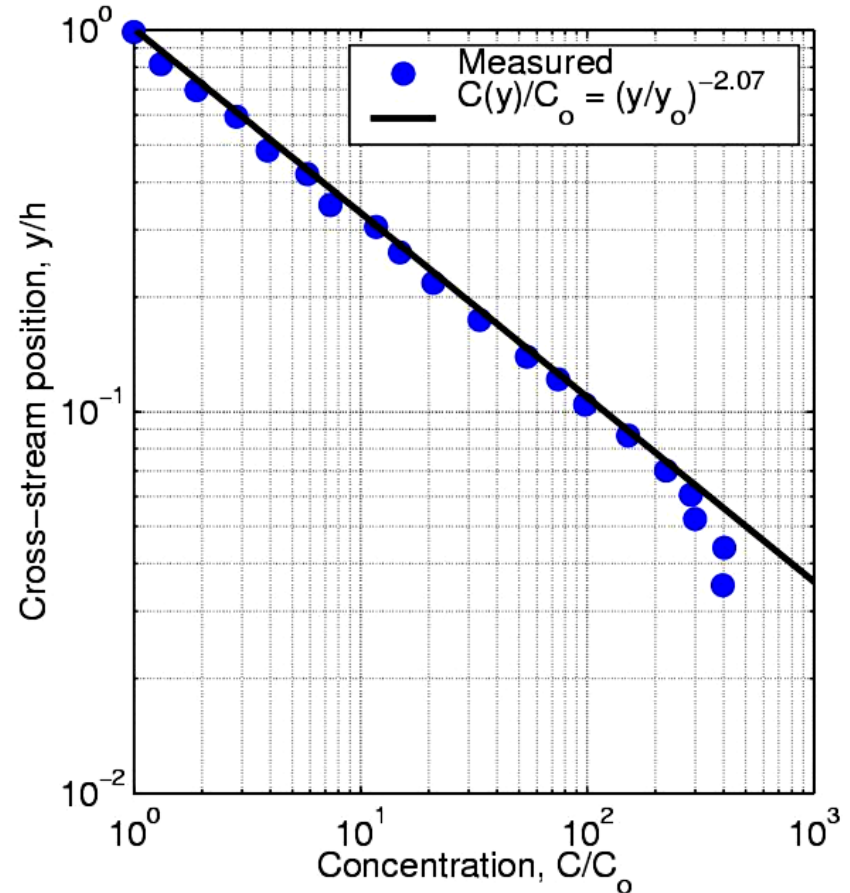
- Concentration follows a power law

- *Equivalent to Rouse distribution for infinite depth*

$$\frac{C(y)}{C(y_o)} = \left( \frac{h-y}{y} \frac{y_o}{h-y_o} \right)^a \approx \left( \frac{y_o}{y} \right)^a$$

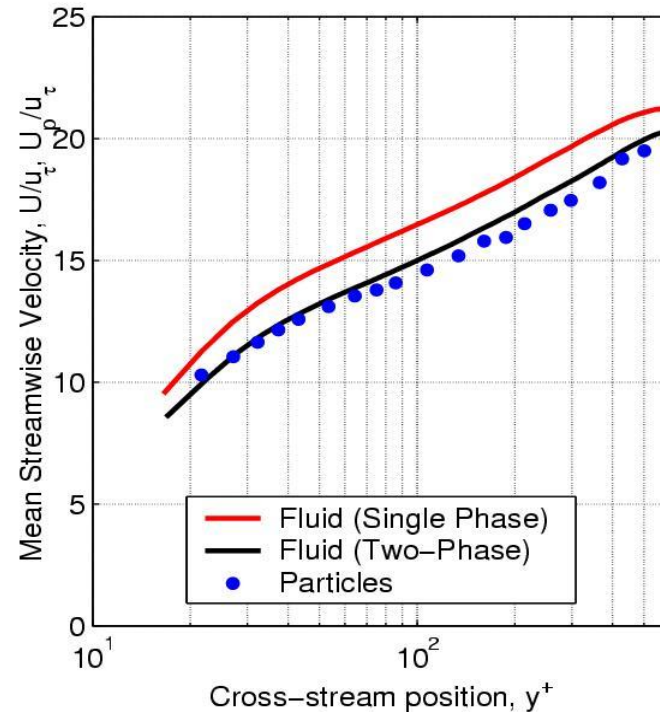
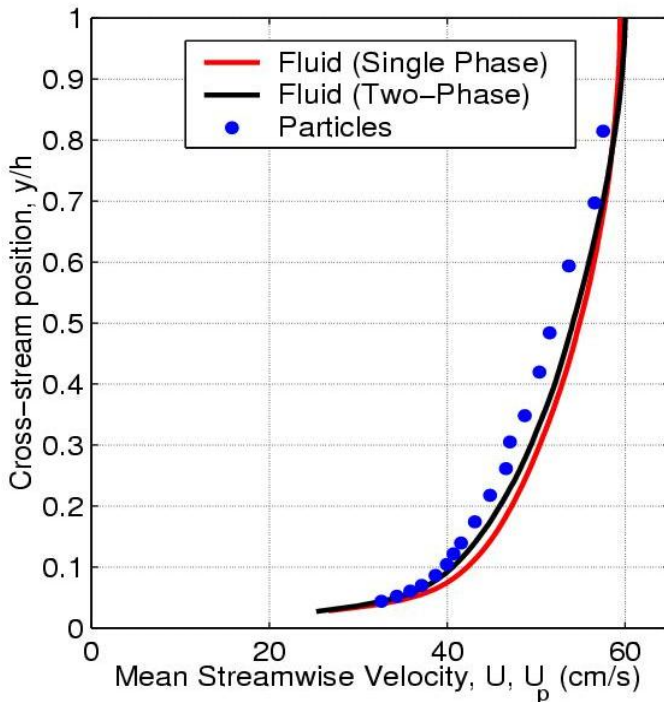
$$a = \frac{v_s}{\kappa u_\tau} = \frac{2.44 \text{ cm/s}}{(0.40)(2.95 \text{ cm/s})} = 2.07$$

- *Based on mixing length theory, but still gives good agreement*



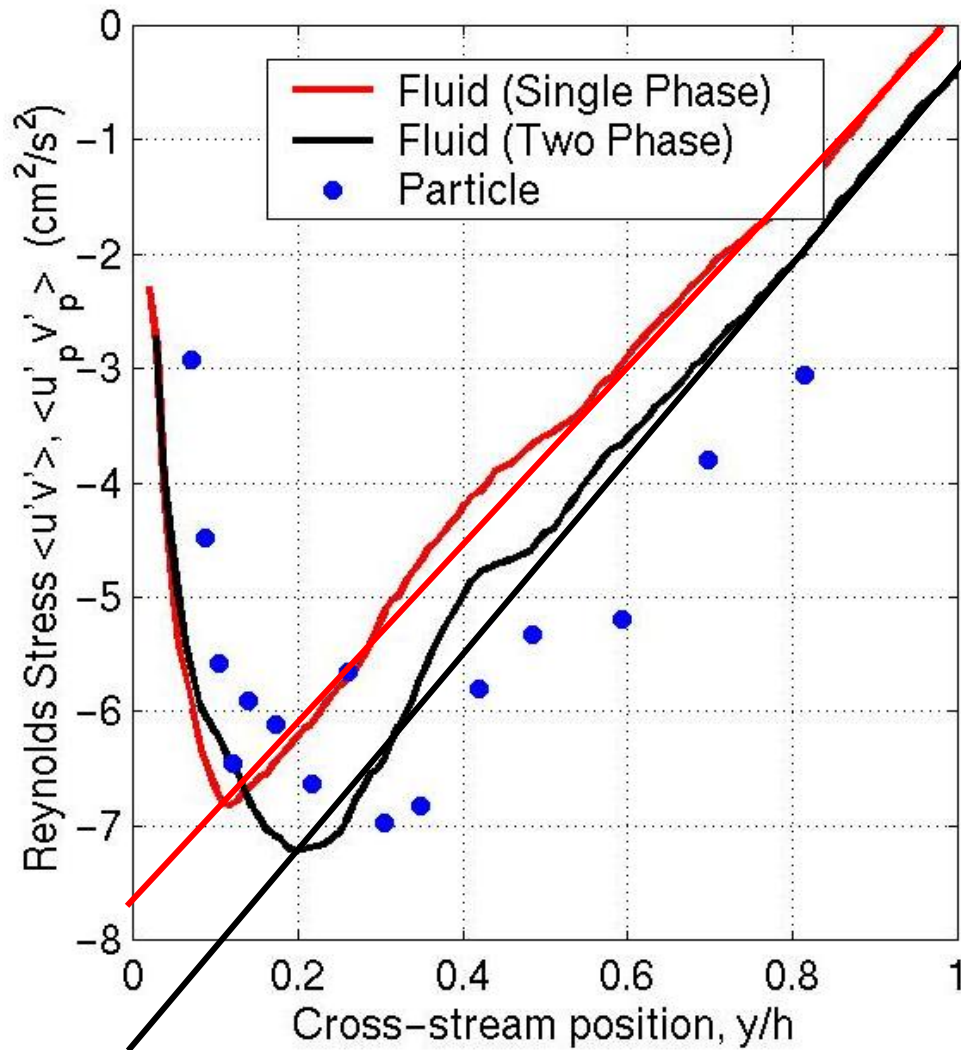


# Mean Velocity



- Particles alter mean fluid profile
  - *Skin friction increased by 7%; qualitatively similar to effect of fixed roughness*
- Particles lag fluid over most of flow
  - *Observed in gas/solid flow (much large Stokes number... likely not same reasons)*
  - *Particles on average reside in slower moving fluid regions?*
    - Reported by Kaftori et al, 1995 for  $\rho_p/\rho_f = 1.05$  (current is heavier  $\sim 2.5$ )
    - Organization of particles to low speed side of structures – a la Wang & Maxey (1993)?
- Particles begin to lead fluid near inner region – transport lag across strong gradient

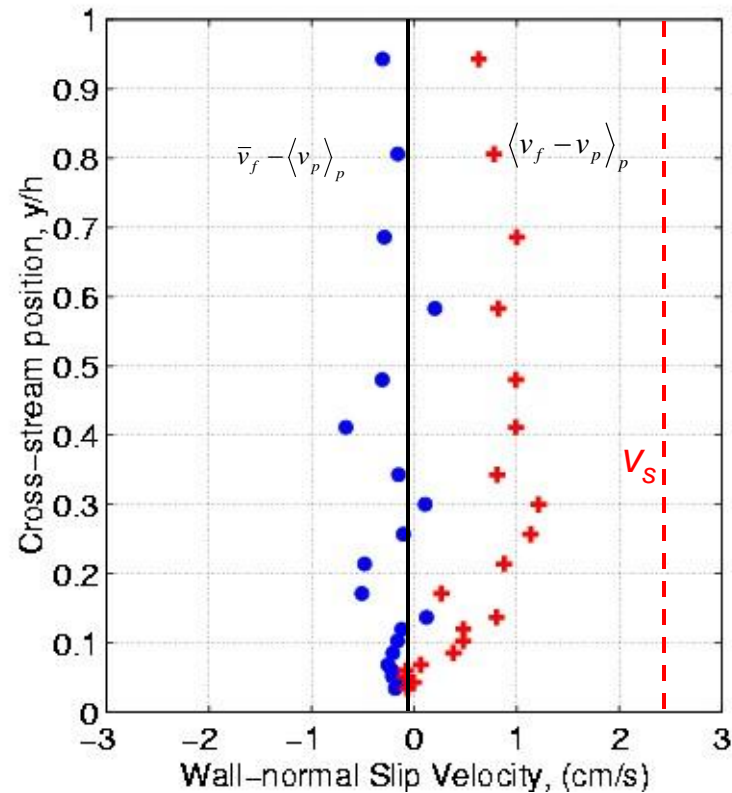
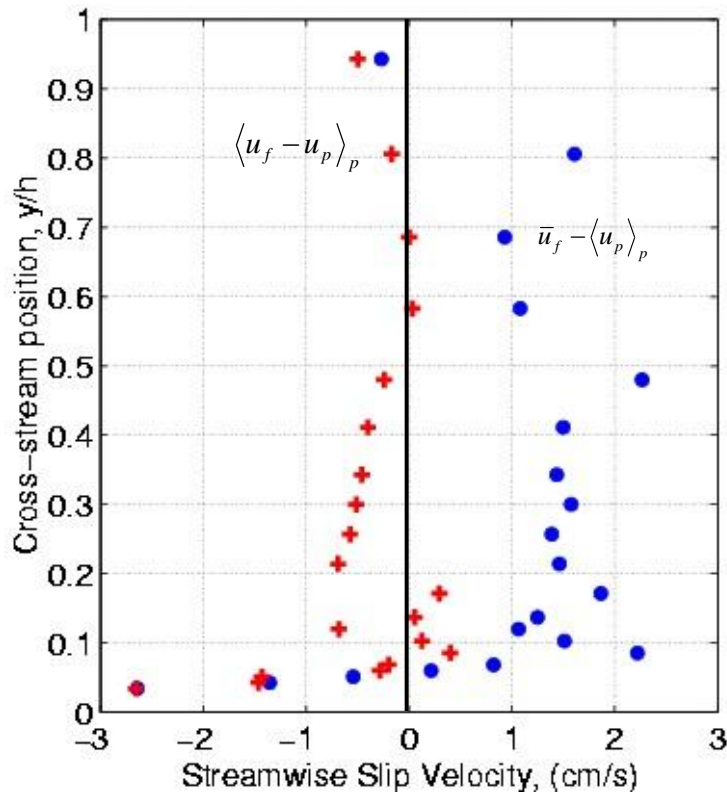
# Two-Phase Flow: Reynolds Stress



- Fluid Reynolds stress maximum displaced further from wall by particle distortion
- Particle Reynolds stress less than fluid close to the wall, greater than the fluid away from the wall.

# Particle Slip Velocity,

$$\bar{u}_f - \langle u_p \rangle_p \quad \langle u_f - u_p \rangle_p$$

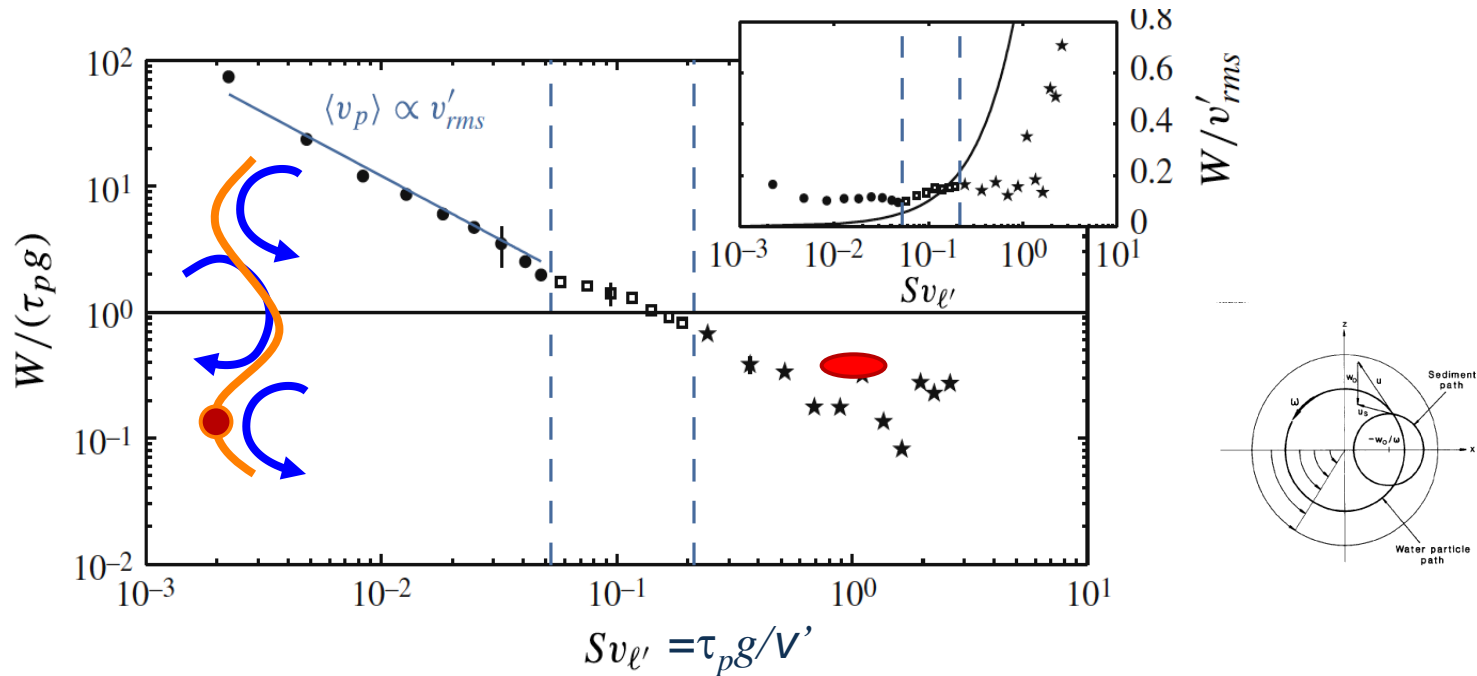


- Streamwise direction
  - Particle-conditioned slip (+) is generally small in outer flow
  - Mean slip (•) and particle conditioned slip are similar in near wall region
- Wall-normal direction
  - Mean slip (•) is negligible
  - Particle-conditioned slip (+) approximately 40% of steady-state settling velocity (2.4 cm/s)

# Effective settling velocity

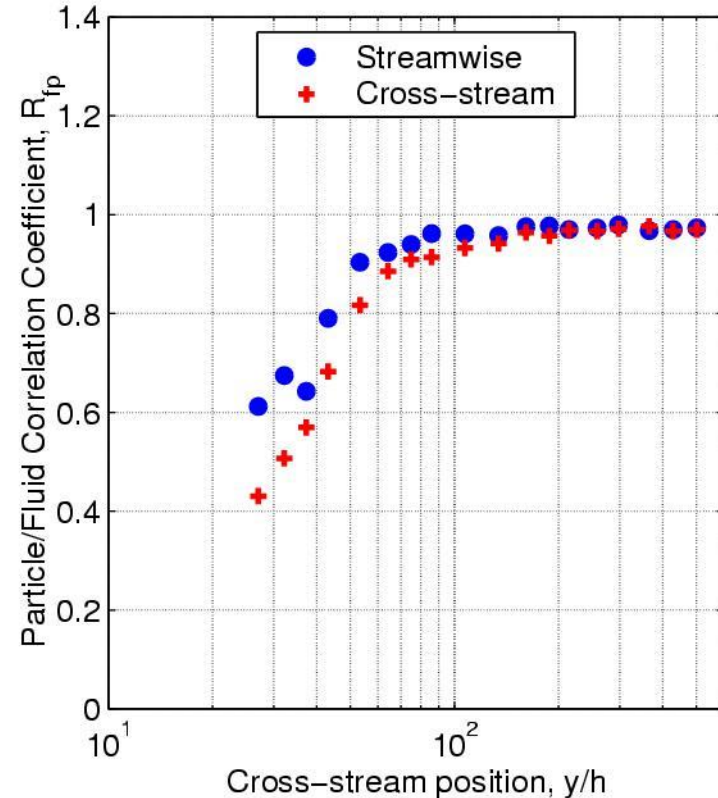
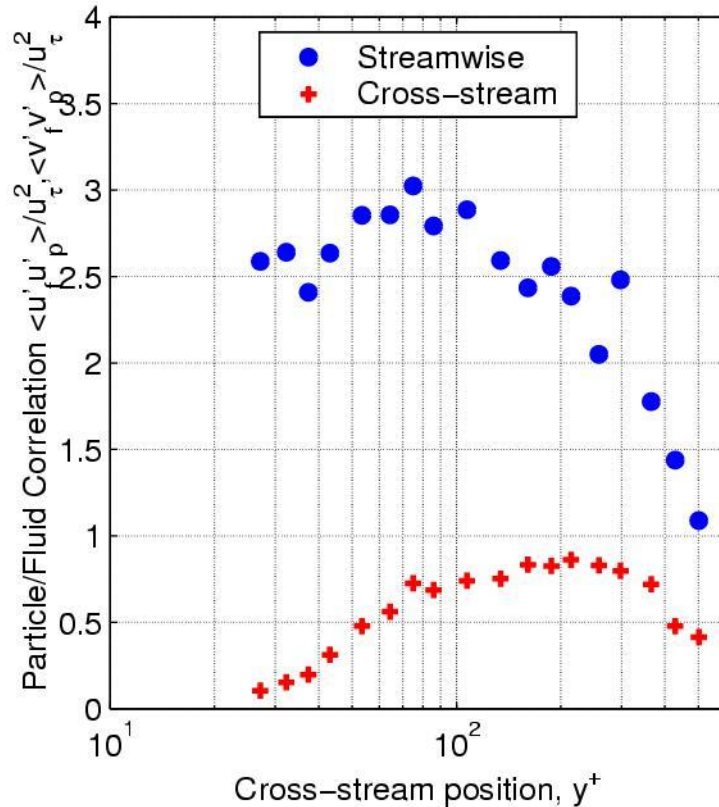
- **Direct measure of settling velocity shows hinder effects**
  - $W/w_0 \sim 0.4$

*G. H. Good, S. Gerashchenko and Z. Warhaft*



- Noted in sediment community by Murray(1970), Nielsen(1993), Kawanisa & Shiozaki (2008)
  - *Enhancement: “fast-tracking”* – Maxey & Corrsin (1986)
  - *Hindered: non-linear drag* – Ho, vortex trapping, loitering

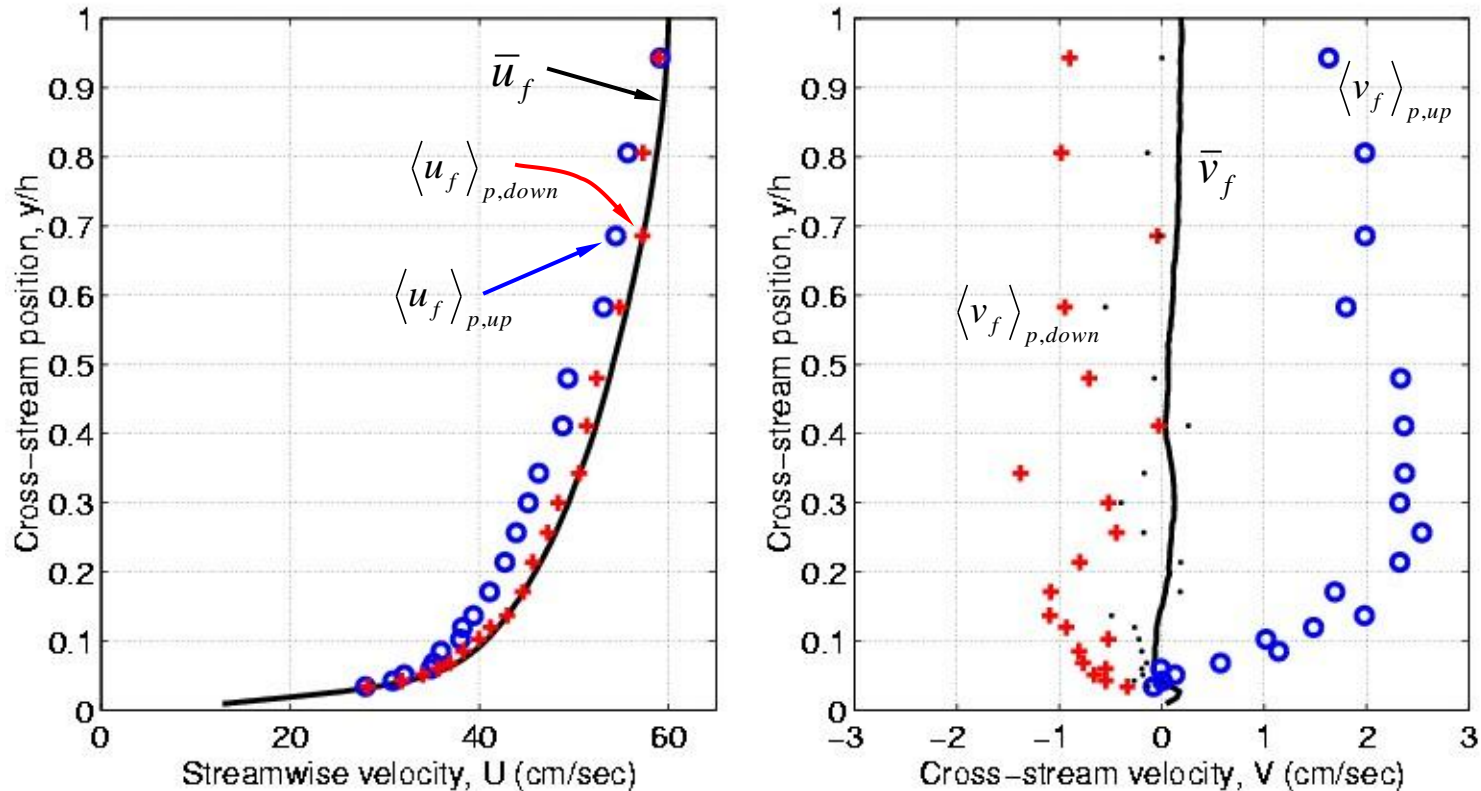
# Two-Phase Flow: Particle/Fluid Correlation



- Particle/Fluid motion highly correlated in outer wall region
  - $R_{fp}$  is high, approximately 1 for  $y^+ > 60$
  - Particles adjust to local flow conditions rapidly



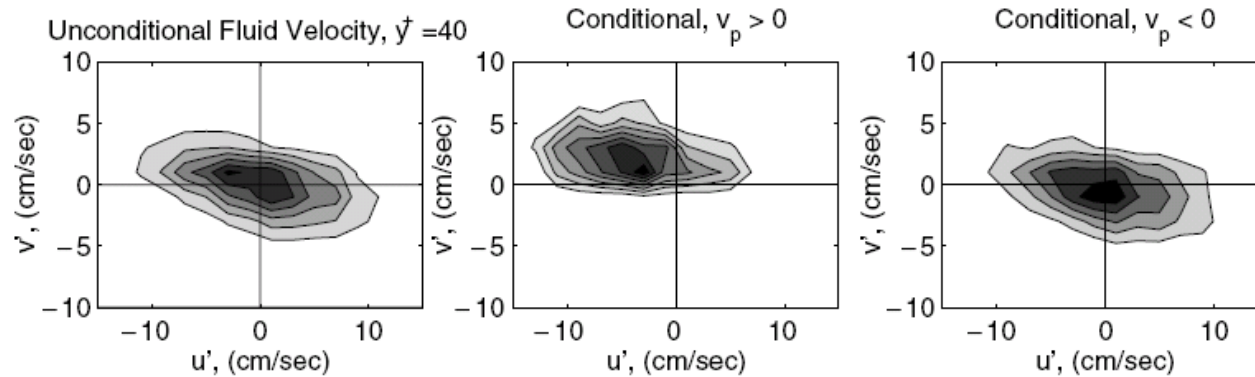
# Particle Conditioned Fluid Velocity Profiles



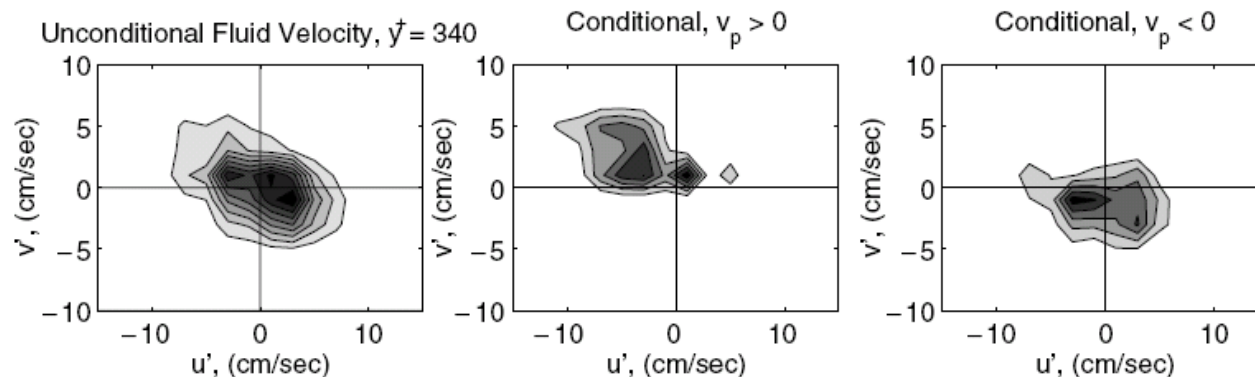
- Average fluid motion at particle locations:
  - *Upward moving particles are in fluid regions moving slower than mean fluid*
  - *Downward moving particles are in fluid regions which on average are the same as the fluid*
  - *Indicates preferential structure interaction of particle suspension*

# Suspension and Sedimentation: Quadrant Analysis

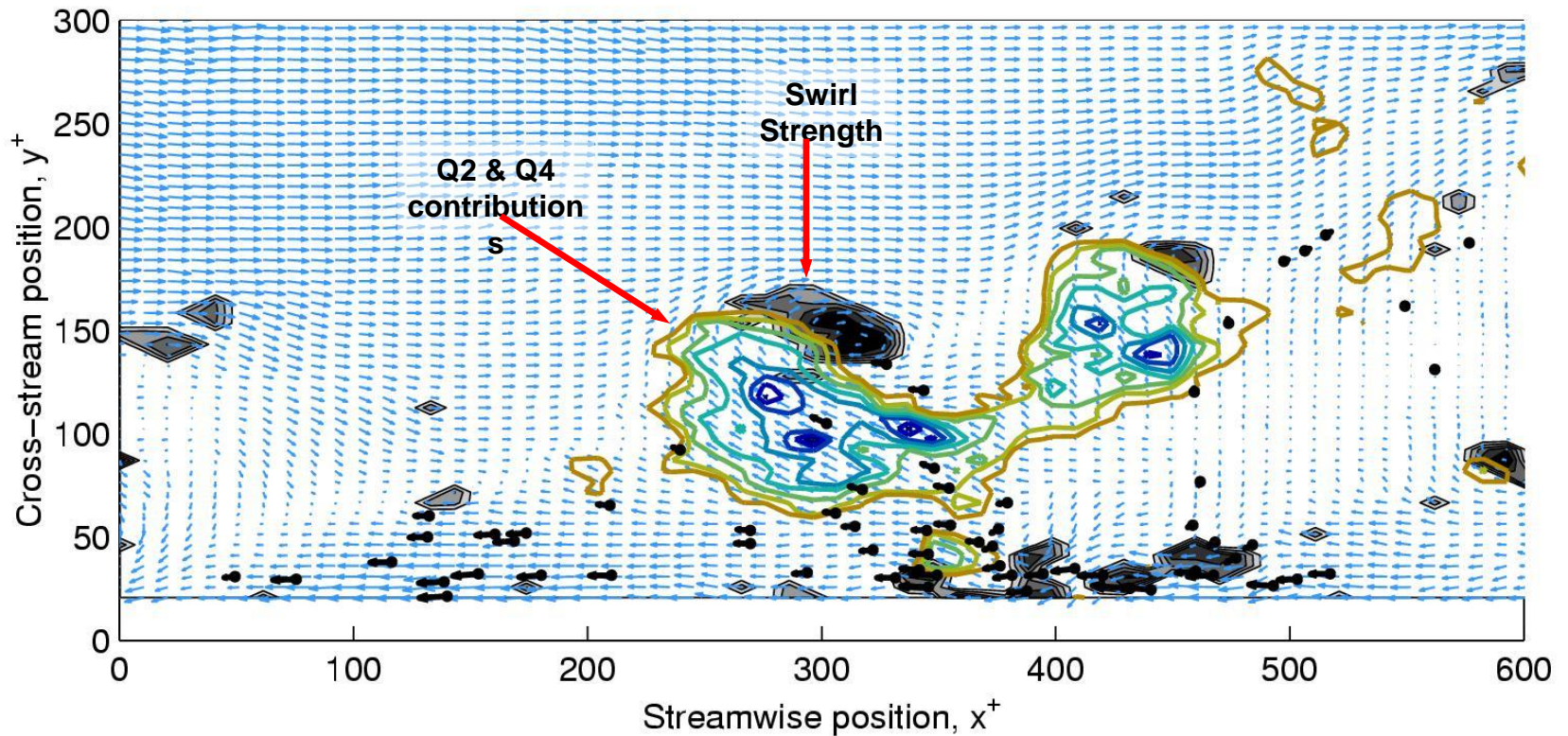
- Conditionally sampled fluid velocity fluctuations
  - *Upward moving particles primarily in quadrant II*
  - *Downward moving particles are almost equally split in quadrant III and IV*



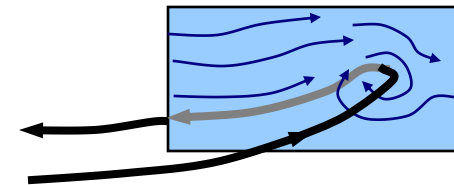
- Persistent behavior
  - *Similar quadrant behavior in far outer region*
  - *Distribution tends towards axisymmetric case in outer region*



# Event structures: Quadrant II hairpin



- **Similar structures found**
  - Appropriate spacing
  - Not as frequent
    - *Re* effects? ( $Re_\theta = 1183$ )
    - *Smaller field of view?*
- **Evidence suggests packets contribute to particle suspension**



# Particle Kinetic Stress

- **Turbulence budget for particle stresses**

- (*Wang, Squires, Simonin, 1998*)

$$\frac{\partial \langle u_i u_j \rangle}{\partial t} + U_{2,m} \frac{\partial \langle u_i u_j \rangle}{\partial x_m} = P_{2,ij} + D_{2,ij} + P_{2,ij}^d + P_{2,ij}^p$$

- Production by mean shear

$$P_{2,ij} = -\langle u_{2,i} u_{2,m} \rangle \frac{\partial U_{2,j}}{\partial x_m} - \langle u_{2,j} u_{2,m} \rangle \frac{\partial U_{2,i}}{\partial x_m}$$

- Transport by fluctuations

$$D_{2,ij} = -\frac{1}{a_2} \frac{\partial}{\partial x_m} \left[ a_2 \langle u_{2,i} u_{2,j} u_{2,m} \rangle \right]$$

- Momentum coupling to fluid
  - (destruction)

$$P_{2,ij}^d = -\left\langle \frac{r_1}{r_2} \frac{3}{2} \frac{C_d}{d} |\mathbf{v}_r| u_{2,i} u_{2,j} \right\rangle_2$$

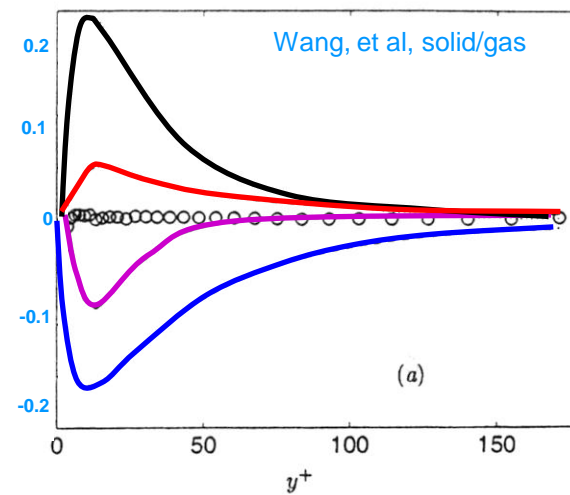
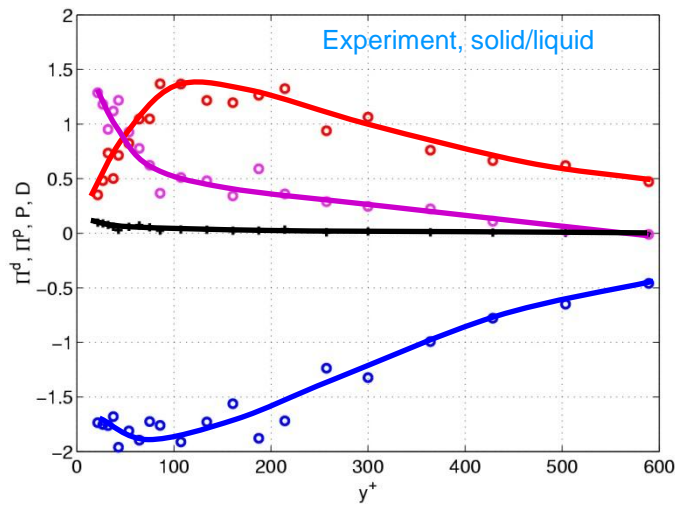
- Momentum coupling to fluid
  - (production)

$$P_{2,ij}^p = \left\langle \frac{r_1}{r_2} \frac{3}{4} \frac{C_d}{d} |\mathbf{v}_r| [u_{1,i} u_{2,j} + u_{1,j} u_{2,i}] \right\rangle_2$$



# Streamwise Particle Kinetic Stress Budget

- **Streamwise Particle/Fluid Coupling:  $\Pi_{2,11}^d, \Pi_{2,11}^p$** 
  - Compare results to Wang, Squires, & Simonin (1998)
    - Gas/solid flow ( $\rho_2/\rho_1=2118$ ),  $Re_\tau = 180$ , No gravity,  $St^+ \sim 700$
    - Computations, all 4 terms are computed; Experiments, all but  $D_{2,ij}$  computed



(—)  $D_{2,ij}$ ; (—)  $\Pi_{2,ij}^d$ ; (—)  $\Pi_{2,ij}^p$ ; (—)  $P_{2,ij}$ ; (o) sum

- Interphase terms are qualitatively similar
  - Similar general shapes,  $\Pi_{11}^d > \Pi_{11}^p$
- Quantitative difference
  - Magnitudes different:  $\Pi_{11}^d / \Pi_{11}^p \sim 1.3$  vs 3, overall magnitudes are 10 to 20 times greater
    - Interphase terms are expected to increase with increased fluid density and decreased  $St^+$
  - Dominant interphase transfer ( $\Pi$ ) greatly diminishes importance of mean shear ( $P$ )
  - Turbulent transport ( $D$ ) has opposite sign because of small shear production ( $P$ )



# Model Approximations

- Model 1 (Simonin, Deutsch & Boivin, 1995)**

- In limit of small  $Re_p \ll 1$ ,  $\tau_{12}^F = \tau_p$ , which is constant

$$\tau_{12}^F = \frac{\rho_2}{\rho_1} \frac{4}{3} \frac{d}{\langle C_D \rangle} \frac{1}{\langle |\mathbf{v}_r| \rangle}$$

$$\Pi_{2,ij}^d = - \left\langle \frac{\rho_1}{\rho_2} \frac{3}{2} \frac{C_d}{d} |\mathbf{v}_r| u_{2,i}'' u_{2,j}'' \right\rangle_2$$

- For finite  $Re_p$ , try to separating  $\tau_{12}^F$

$$P_{2,ij}^p \gg \frac{1}{t_{12}^F} \left[ \langle u_{1,i}^{\mathcal{C}} u_{2,j}^{\mathcal{C}} \rangle + \langle u_{2,i}^{\mathcal{C}} u_{1,j}^{\mathcal{C}} \rangle \right]$$

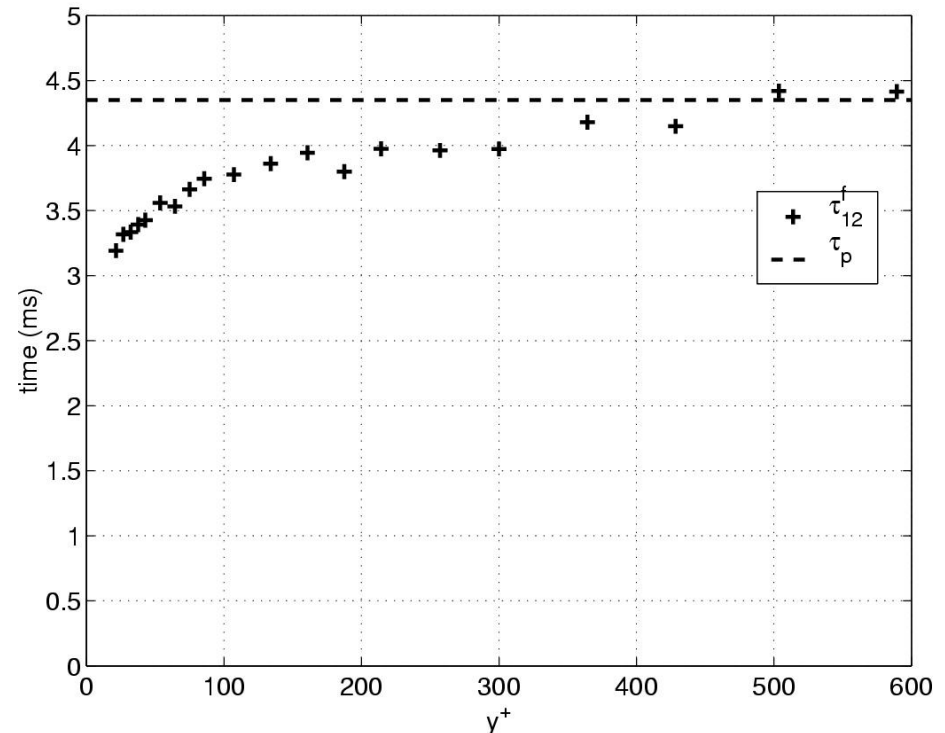
$$\Pi_{2,ij}^d \approx - \frac{2}{\tau_{12}^F} \langle u_{2,i}'' u_{2,j}'' \rangle$$

- Model 2**

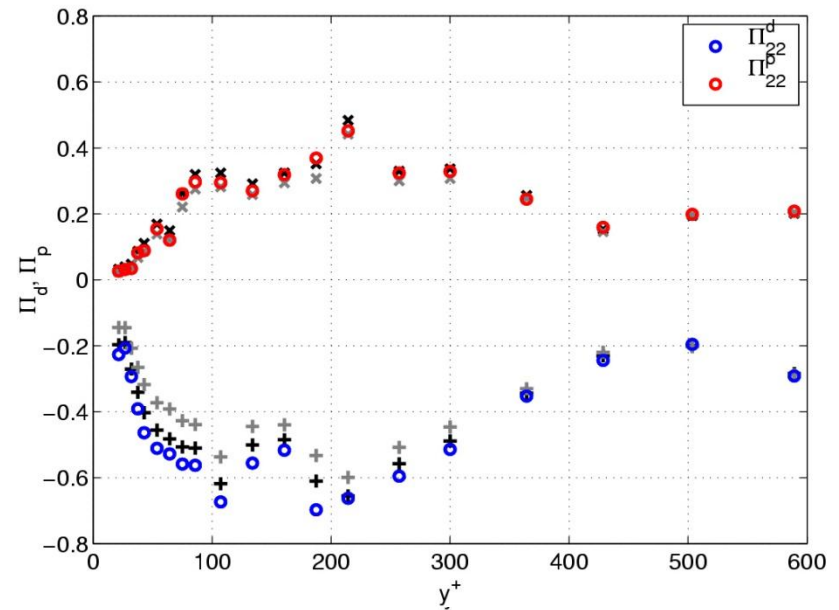
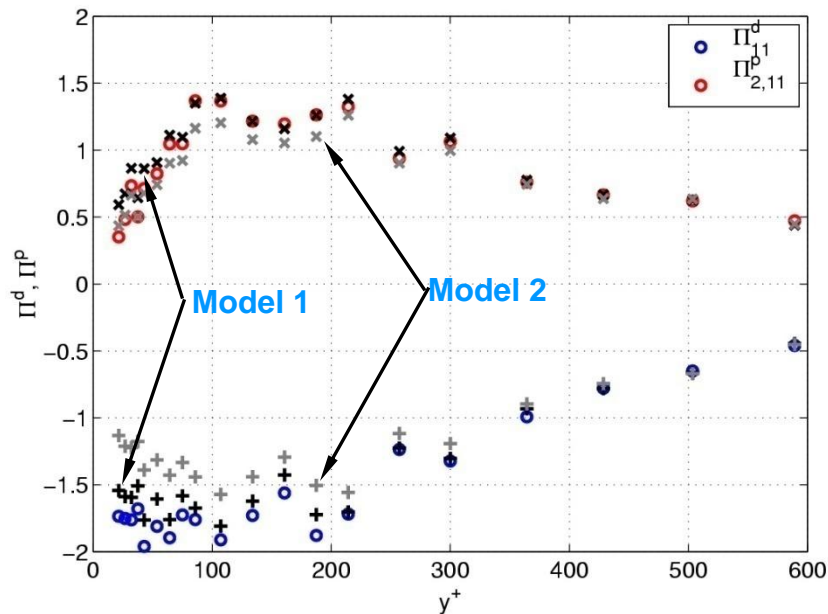
- Use  $\tau_p$  instead of local  $\tau_{12}^F$

$$P_{2,ij}^p \gg \frac{1}{t_p} \left[ \langle u_{1,i}^{\mathcal{C}} u_{2,j}^{\mathcal{C}} \rangle + \langle u_{2,i}^{\mathcal{C}} u_{1,j}^{\mathcal{C}} \rangle \right]$$

$$\Pi_{2,ij}^d \approx - \frac{2}{\tau_p} \langle u_{2,i}'' u_{2,j}'' \rangle$$



# Particle Stress Model Comparison



- **Model 1**

- $\Pi_{ij}^p$  agrees within 5% for  $y^+ > 50$ , overestimates ~30% near wall
- $\Pi_{11}^d$  agrees within 10% or better, consistently underestimates near the wall

- **Model 2**

- OK in outer region where  $Re_p$  is small
- Up to 30% underestimate relative to Model 1 near wall

## Part II: Dust suspension by impinging jets



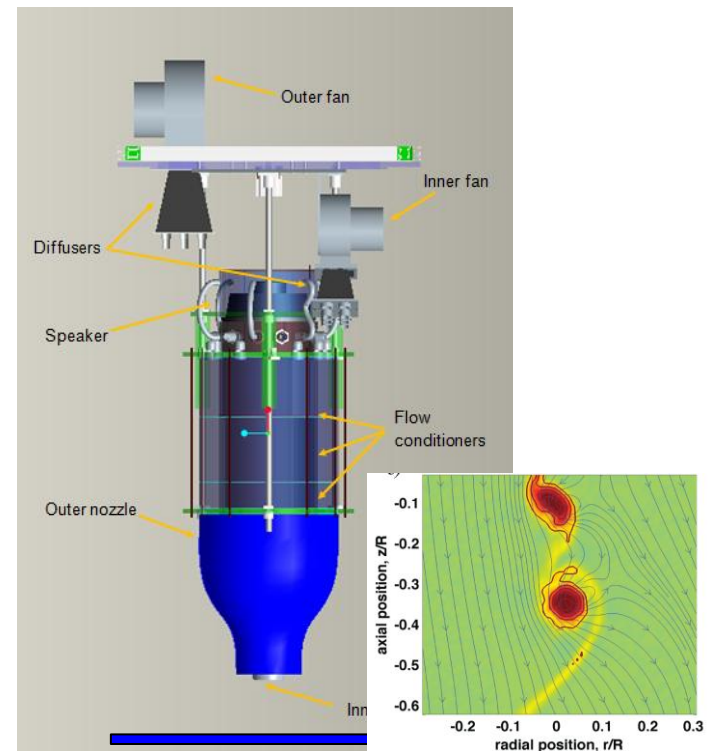
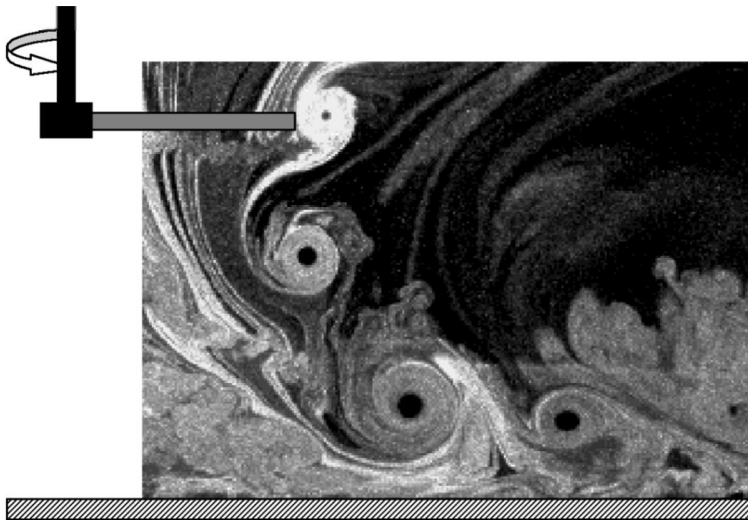
# Interesting detail...



Photograph by Zoltan Szoboszlay of NASA Ames Flight Research Center

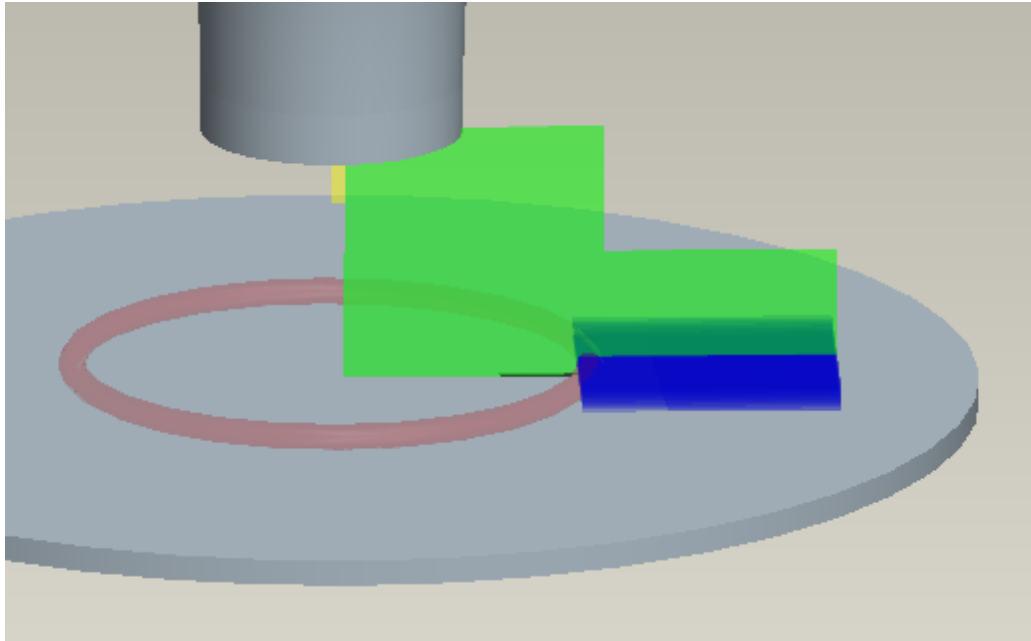
# Experimental Set up

- **Mimic rotorcraft in ground effect with simple prototype flow**
  - Forced impinging jet
    - *Maintain intense vortex structure embedded within stagnation flow*
    - *Does not retain helical nature of rotorcraft wake*





# Current Imaging Planes



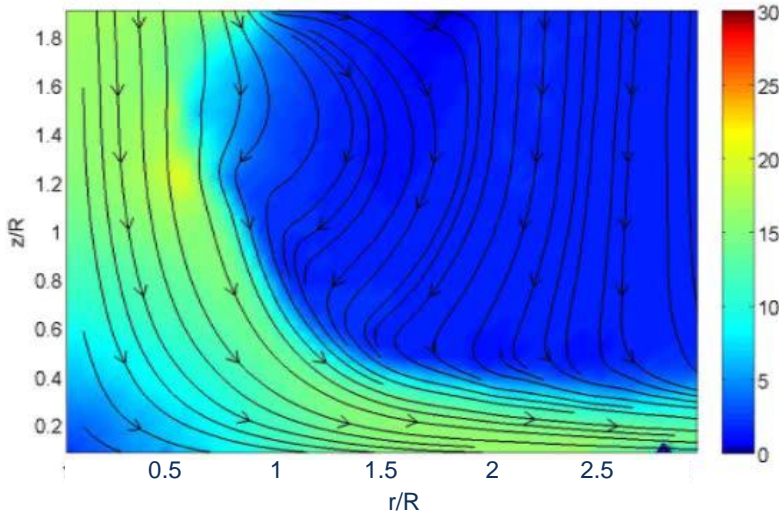
- **Three vertical planes (PIV)**
  - Vortex ring trajectory
  - Vortex ring development
  - Vortex ring breakdown
- **Stacked horizontal planes (Stereo PIV)**
  - Measure breakdown at different heights on the vortex ring
- **Data Collection**
  - 4 MP sensor
  - 37 phase angles
  - 50 image pairs per phase angle
    - *(high order statistics not fully converged)*

Laser Sheet width ~ 1.5 mm

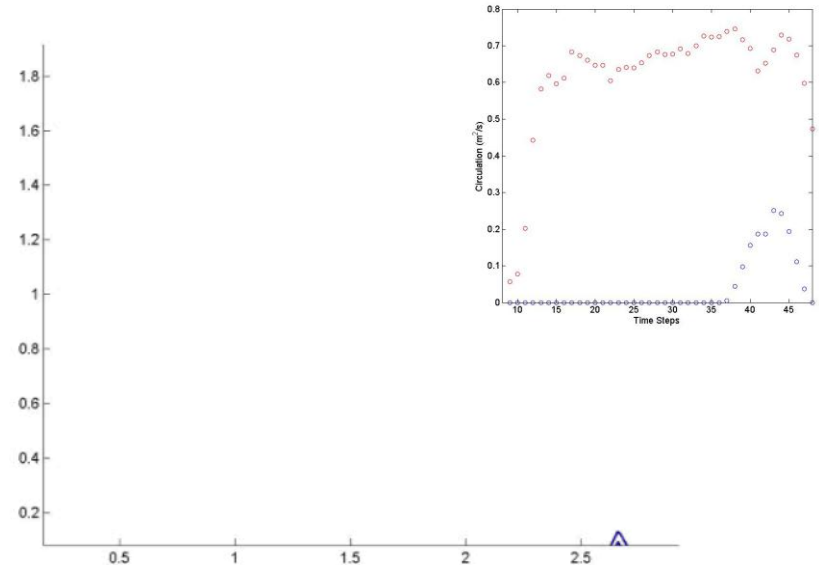
# Chosen Waveform Imaging

- **Single phase characterization**

- 13.3 ms sine wave pulse, repeated at 2 Hz interval,  $V_{\text{jet}} \sim 10$  m/s
- $h/D_j = 1$  ( $D_j = 10$  cm)



*Ensemble Average Velocity*

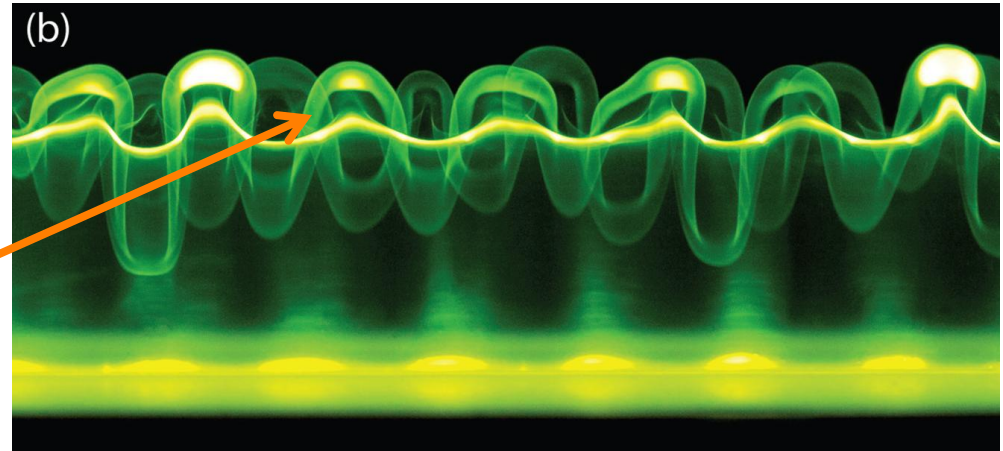


*Vorticity Contours*

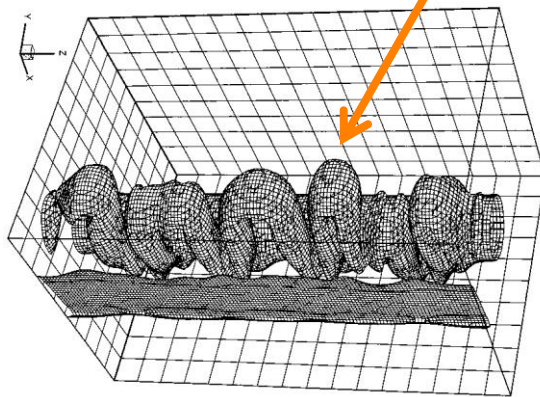
- Vortex formation highly repeatable up to point of destabilization during wall interaction
- Nominal strength,  $\Gamma \sim 0.7$  m<sup>2</sup>/s,  $Re = \Gamma/\nu \sim 50,000$

# Secondary Vortex Instability

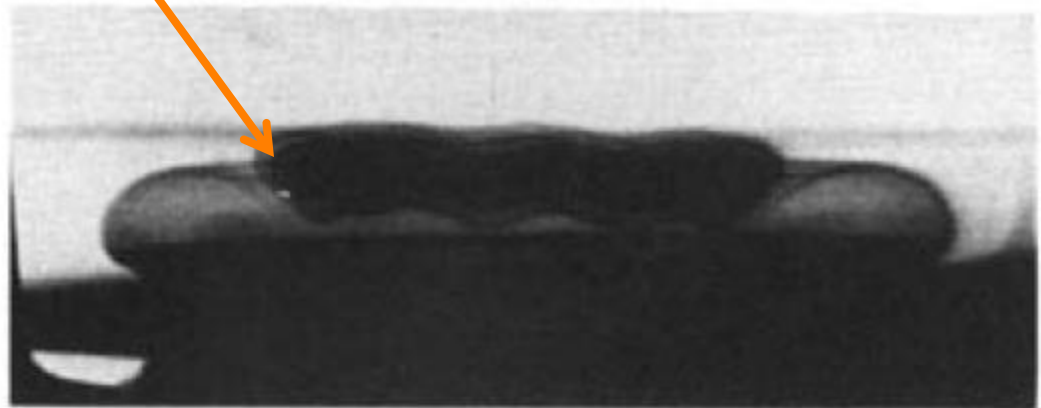
- Azimuthally unstable wrapping of the secondary vortex



*Harris, Miller, and Williamson, Phys. Fluids 2010*



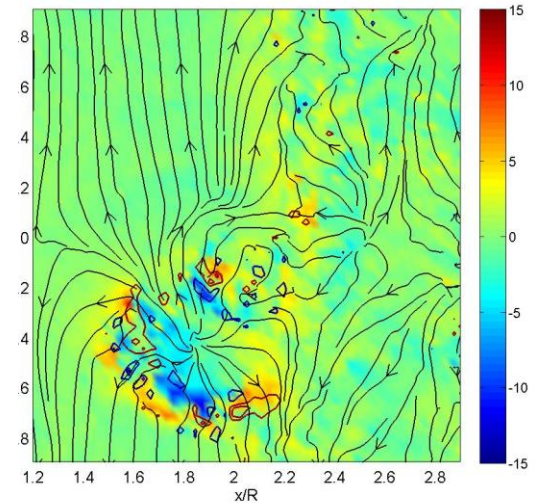
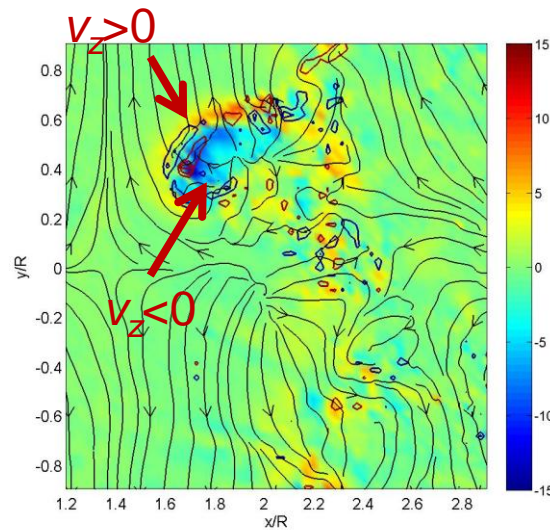
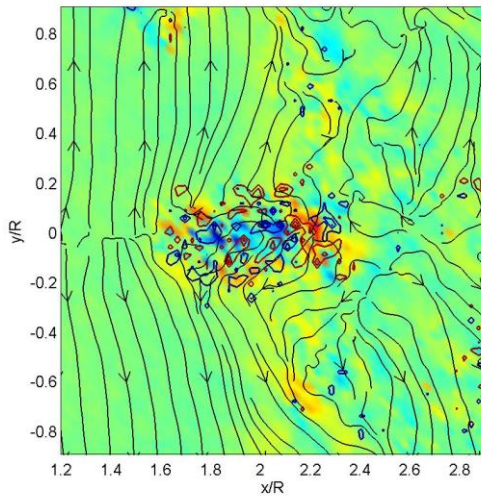
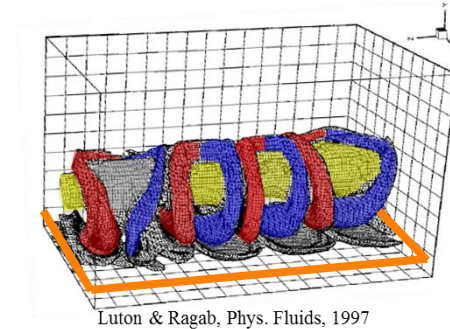
*Luton and Ragab, Phys. Fluids 1997*



*Walker & Smith J., Fluid Mech. 1987*

# Instantaneous Breakdown Imaging

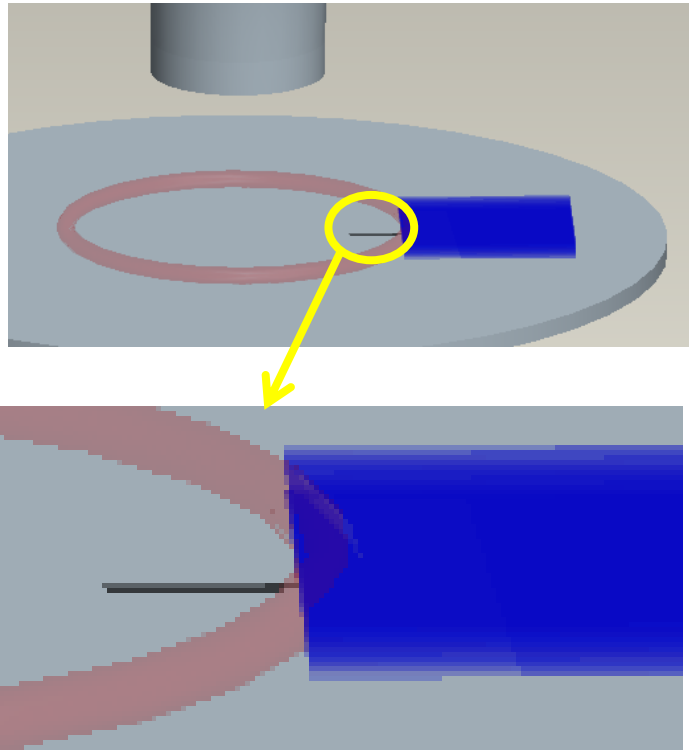
- Consistent structures of out-of-plane velocity
- Azimuthally unstable
- Instantaneous snapshots:



1mm above ground plane

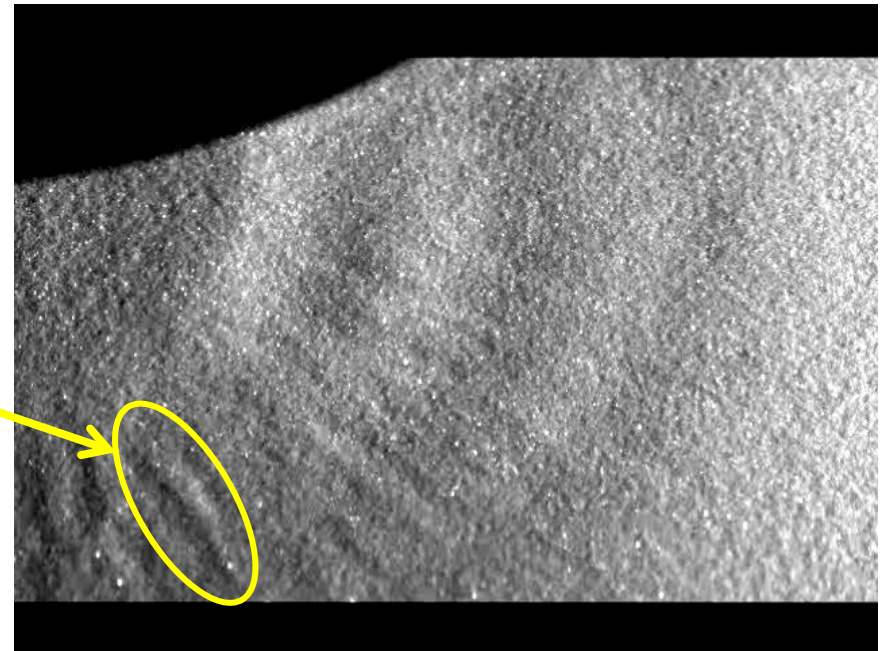


# Axial Fence Introduction



- **Wrapping instigated by examining the influence of small radial “fence”**
  - Small height:  $d/D_{\text{vortex}} \sim 0.05$
  - Length,  $l/D_{\text{vortex}} \sim 1$
- Current data extracted from  $z/R = 0.025$  only
- Fence-like structures occur in brownout flow

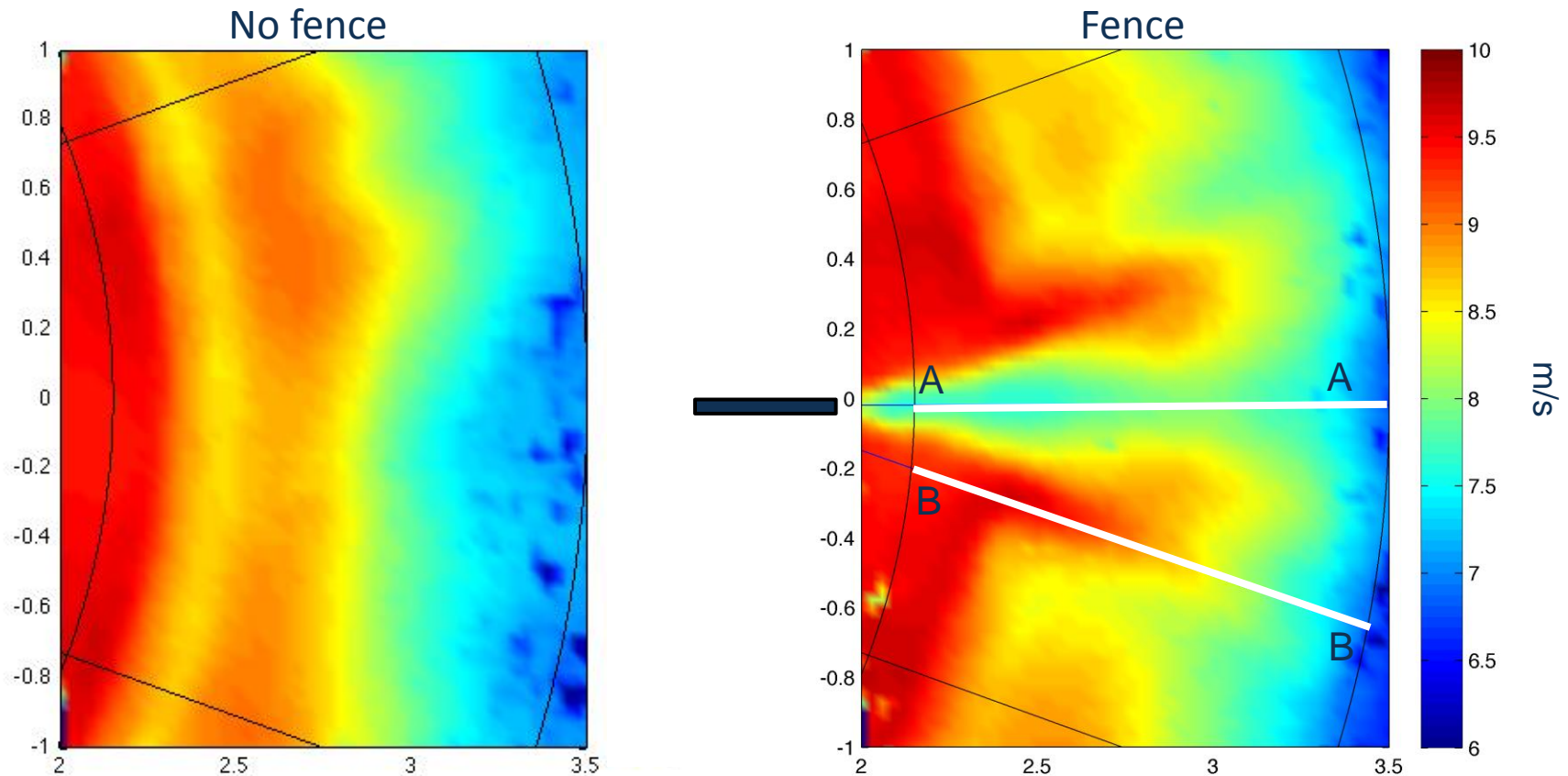
Naturally occurring radial fence.  
Sediment collisional instability?





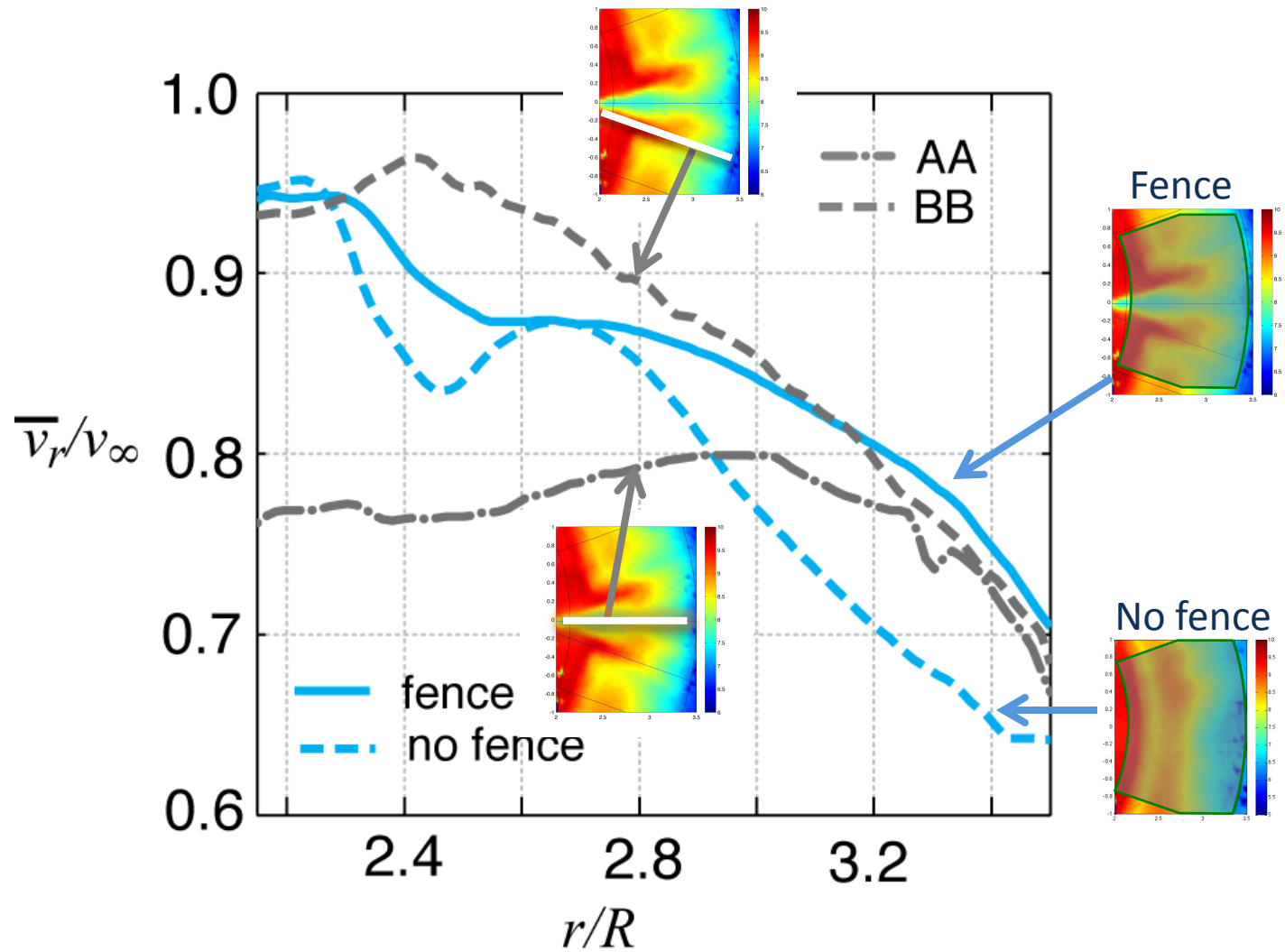
# Time-Average Radial Velocity Fields

$$f(r, f, z, t) = \overbrace{\bar{f}(r, f, z)}^{\text{Time-average}} + \overbrace{\tilde{f}(r, f, z, t/T)}^{\text{periodic}} + \overbrace{f^{\text{st}}(r, f, z, t)}^{\text{stochastic}}$$



- AA and BB illustrate the high- and low-speed streak region

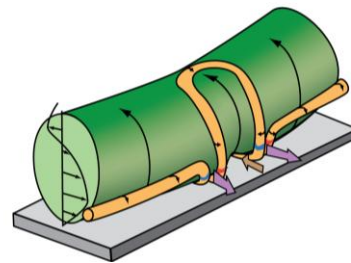
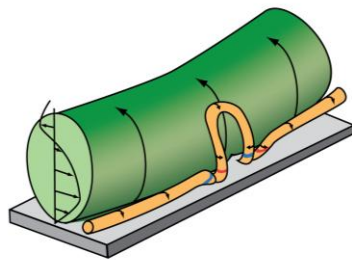
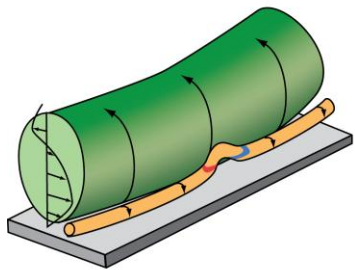
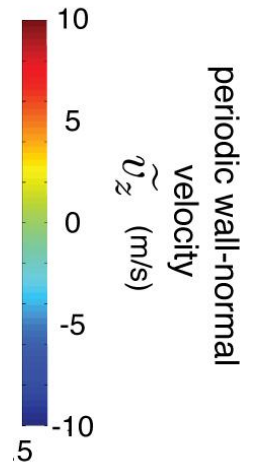
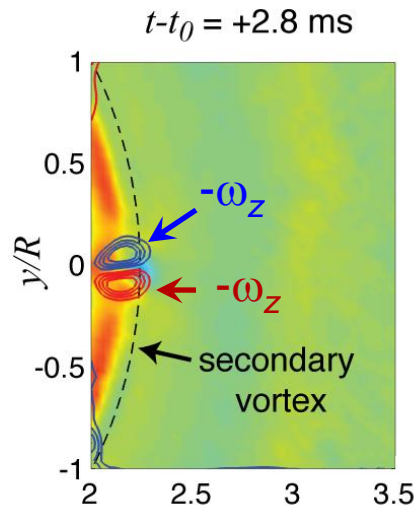
# Average Radial Velocity Fields



- Peak radial velocity similar in early near-wall flow, up to +15% downstream for fence
- High-speed streak 25% greater than low-speed region in early wake, similar downstream

# Near-wall Evolution

- **Near wall primary & secondary vortex signature**
  - Wall-normal velocity and wall-normal vorticity



# Periodic vs. Stochastic Radial Stress

- **Periodic stresses are up to order of magnitude larger**
- **Stochastic variations become dominant past  $r/R > 3$**



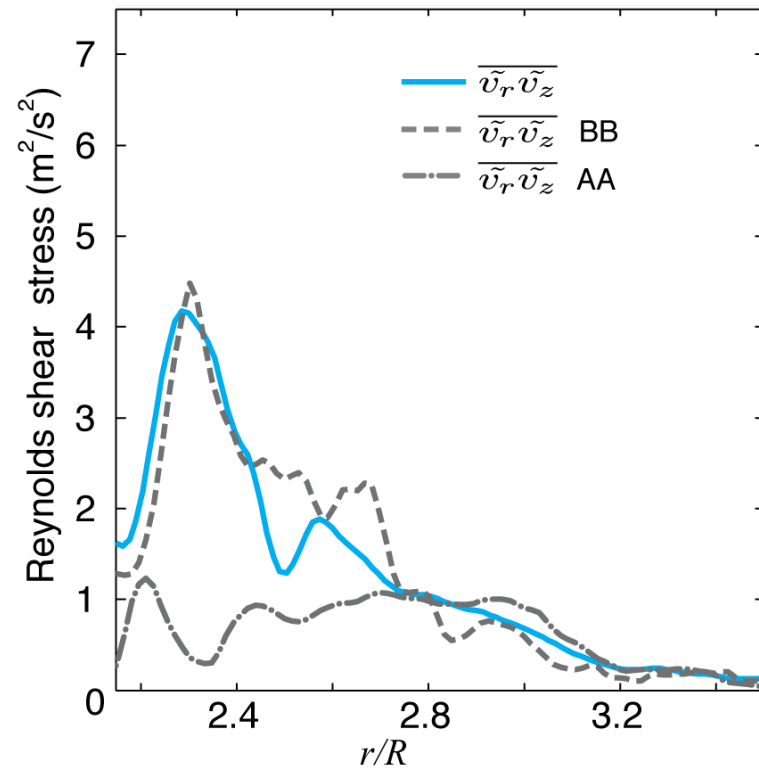
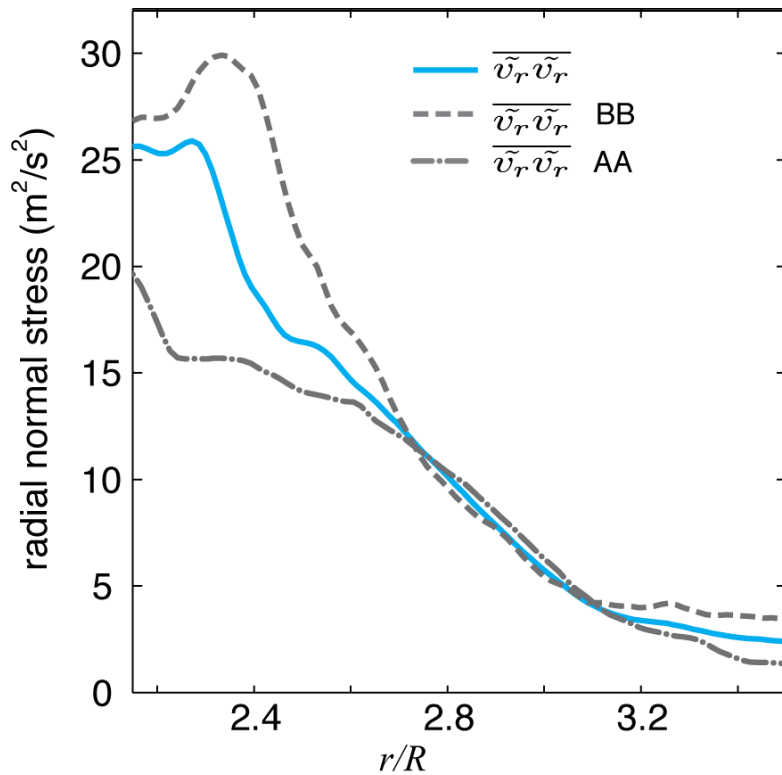
# Reynolds Shear Stresses

- **Radial stresses are up to 2.5 times larger than Reynolds stresses**





# Profiles of Turbulent Stress



## Observations:

- Radial normal stress ( $v_r v_r$ ) typically 3 to 10x  $r$ - $z$  shear stress ( $v_r v_z$ )
  - *Near wall location restricts  $v_z$  magnitude, also normal stress is + only*
- Presence of fence temporarily enhances time-average of fluctuating stress
- Coherent stress dominates for  $r/R < 3$  (closest approach  $r/R \sim 2$ )
- Stress in high-speed region can be 2x that in low-speed region

# Experimental Conditions

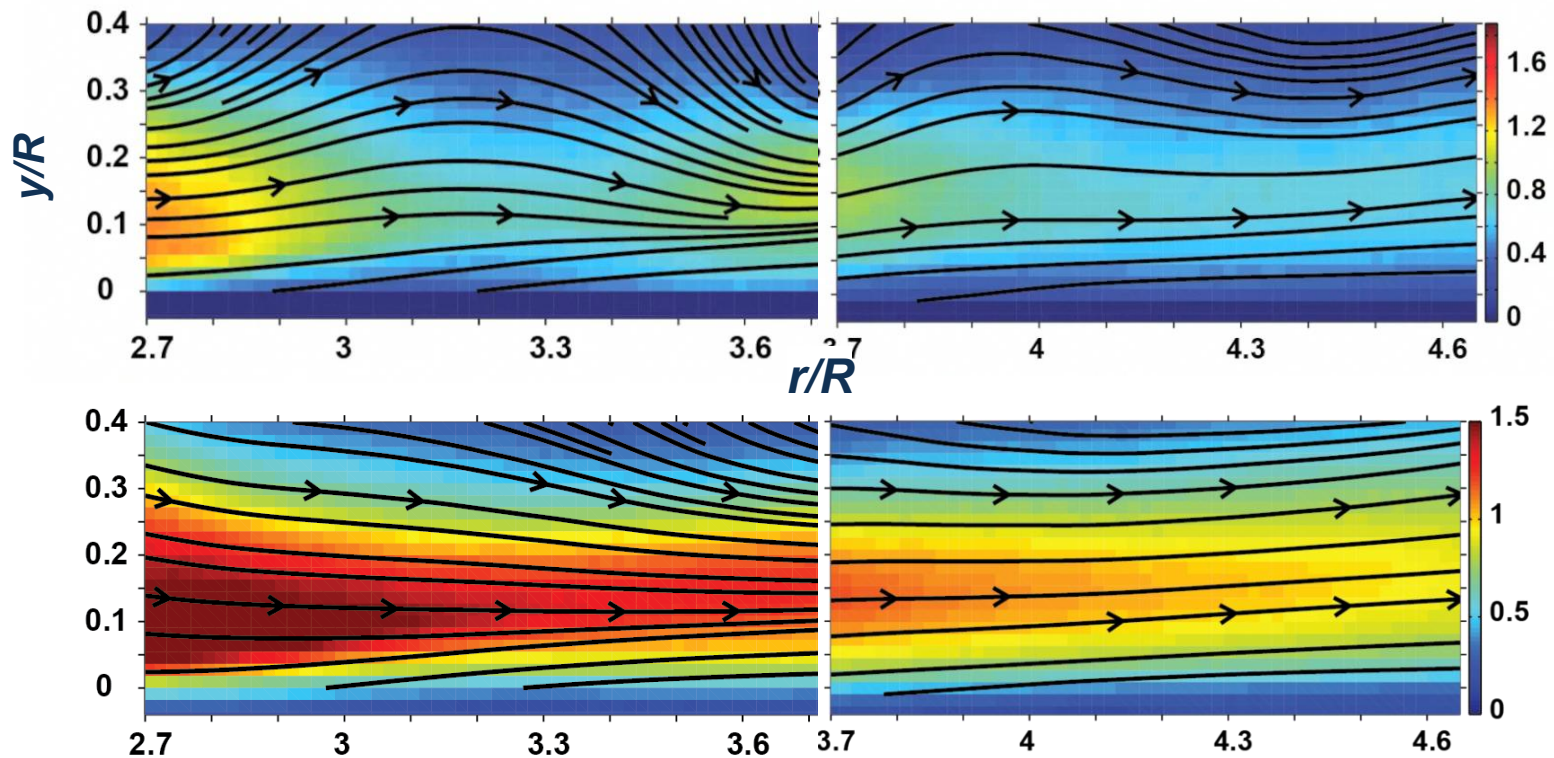
**Table 1** Flow Conditions and particle characteristics

Nozzle radius, $R$ (cm)	5
Mean jet exit velocity, $V_0$ ( $\text{ms}^{-1}$ )	4.1
Forcing frequency, $n$ (Hz)	50
Velocity fluctuation amplitude, $\Delta V$ ( $\text{ms}^{-1}$ )	$\pm 4$
Fluid density, $\rho_f$ ( $\text{kgm}^{-3}$ )	1.2
Kinematic Viscosity, $\nu$ ( $\text{m}^2\text{s}^{-1}$ )	$1.56 \times 10^{-5}$
Particle density, $\rho_p$ ( $\text{kgm}^{-3}$ )	2500
Particle mean diameter, $d_p$ ( $\mu\text{m}$ )	50
Size range ( $\mu\text{m}$ )	45-63
Thickness of the sediment bed (cm)	1.2
Standoff height (cm)	10
Stokes number based on vortex core size	15

$$St = \frac{\tau_p}{\tau_f} \quad \tau_p = \frac{\rho_p d_p^2}{\rho_f 18\nu}$$

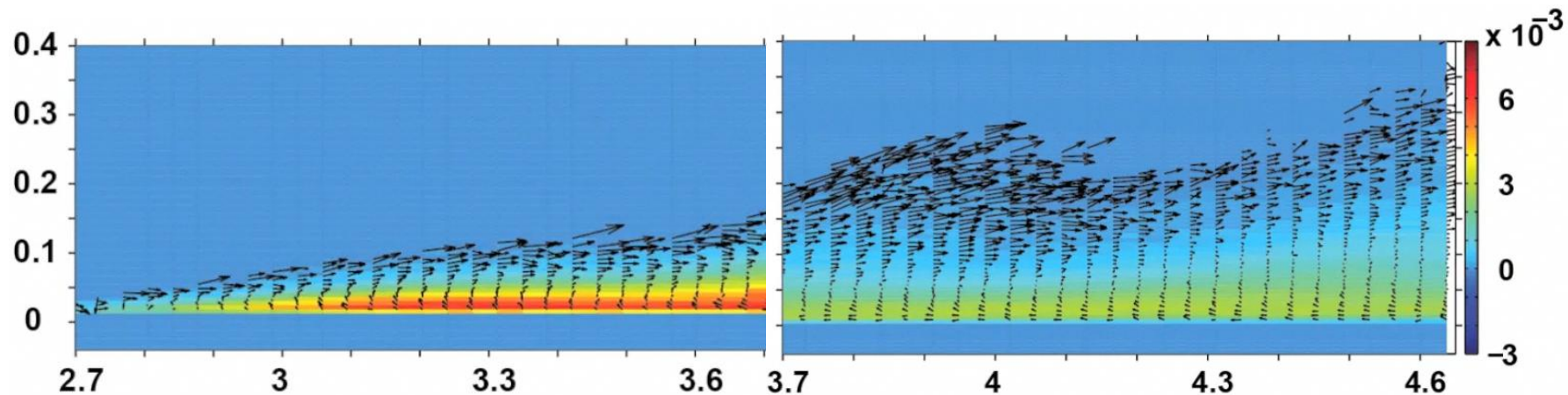
# Two-phase conditions: Fluid Velocity

- **Ensemble-averaged two-phase flow is similar to single-phase**
  - Increased variability in vortex-wall interaction
  - Secondary vortex is not visible (but may be present)
  - Mean flow is in form of strong wall jet



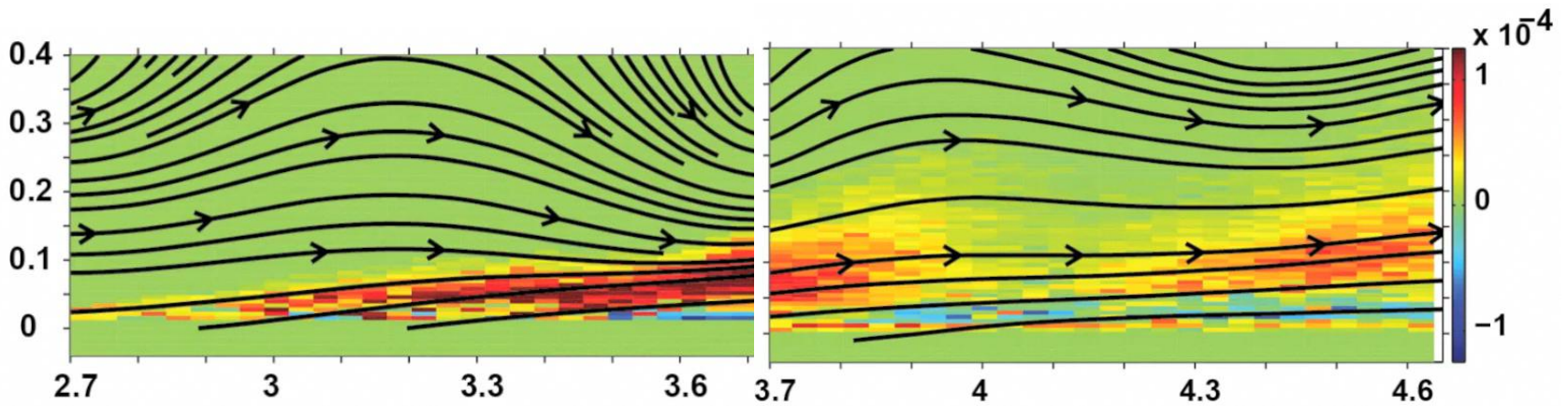
# Particle Concentration & Slip vector

- **The evolution of the suspended load**
  - Predominantly radial scouring along the ground in upstream plane
  - Concentration is highest at the point of closest vortex approach
  - Slip velocity  $\langle u_f - u_p \rangle$  is directed radially outward in outer flow and radially inward close to the ground
    - *Greater suspension heights in downstream plane*
    - *Slip magnitude is larger in downstream plane*



# Vertical Flux

- Unsteady transport into/within suspended load



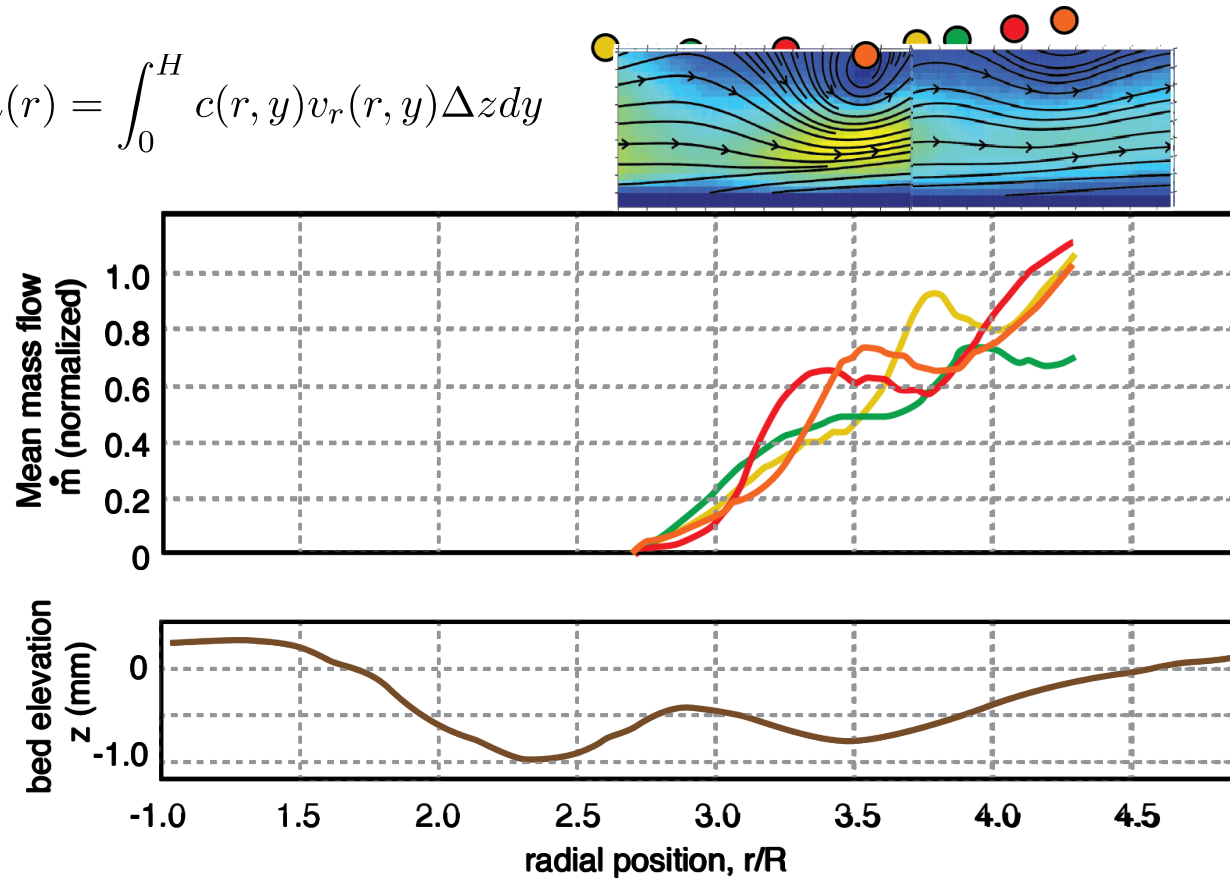


# Horizontal Flux

- **Evolution of suspended/saltating flow**

- observed by change in transported horizontal mass flow rate:

$$\dot{m}(r) = \int_0^H c(r, y) v_r(r, y) \Delta z dy$$



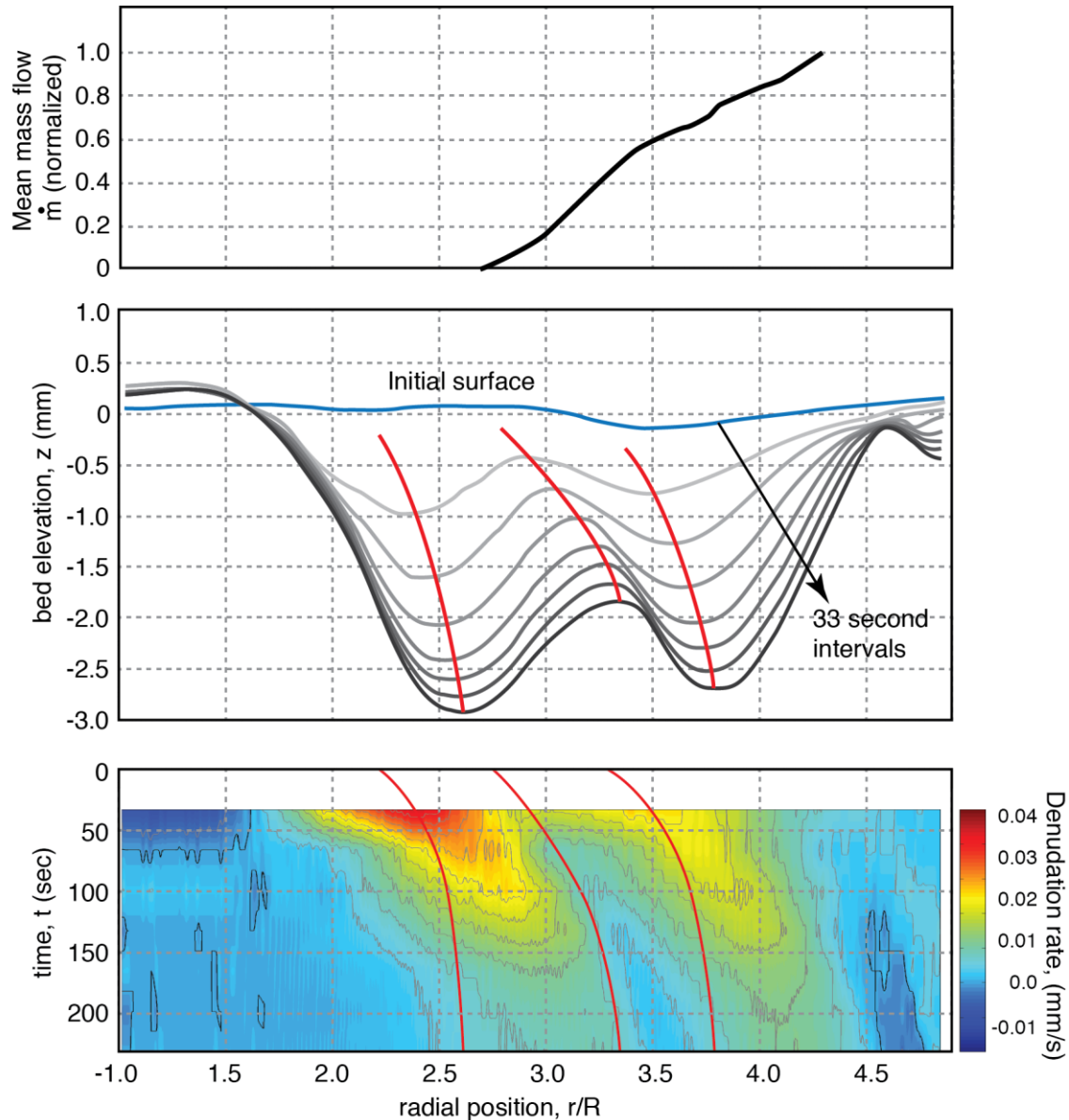
- Sediment waves forced by strong vortical surface flow
- Suspension strongest following first crest

# Bed form evolution

- **Following evolution:**

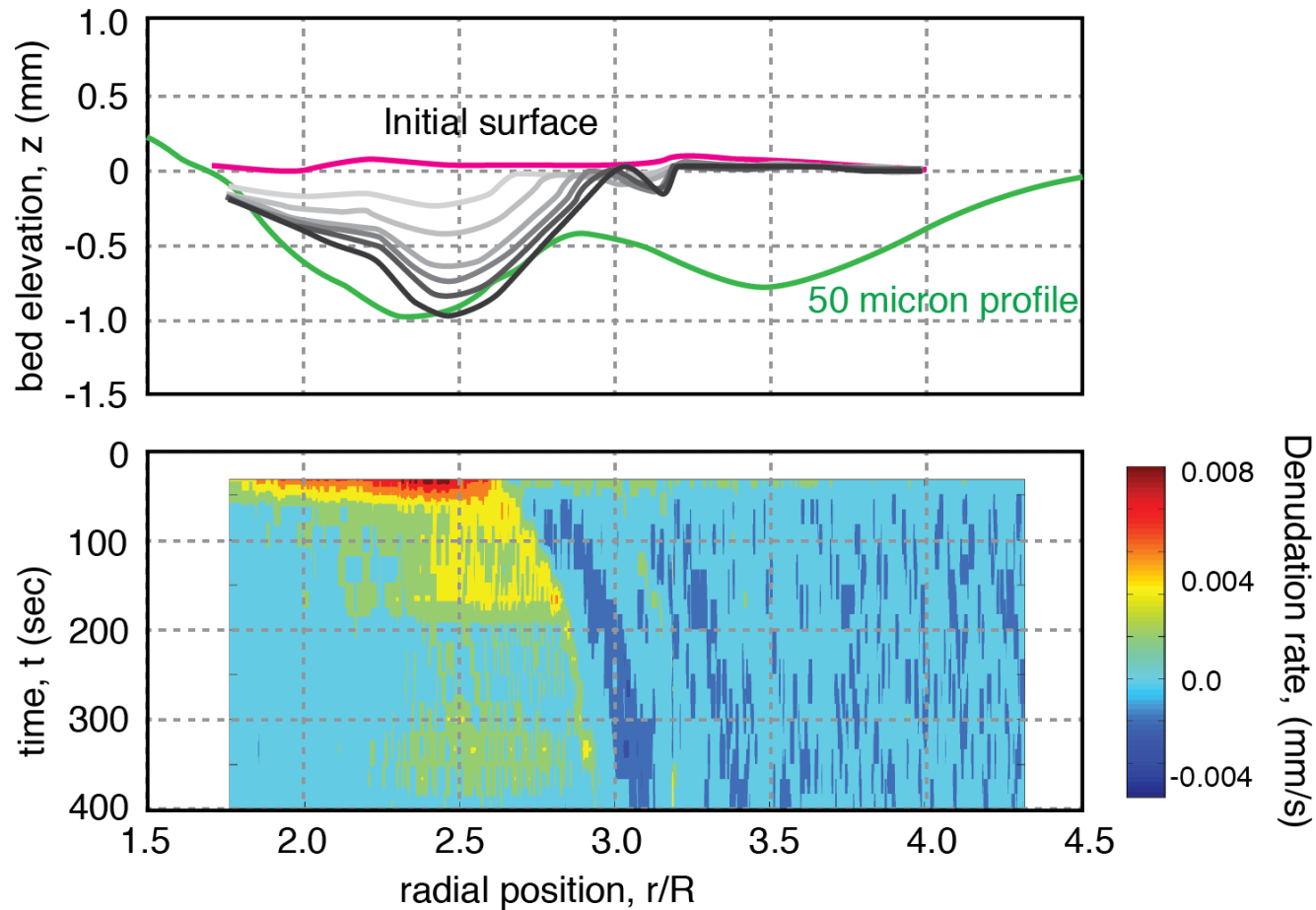
- Two ripples quickly form and deepen, and move downstream
- Erosion rate starts high, and then gradually relaxes

- **What controls the wavelength?**



# Bed forms with larger particles

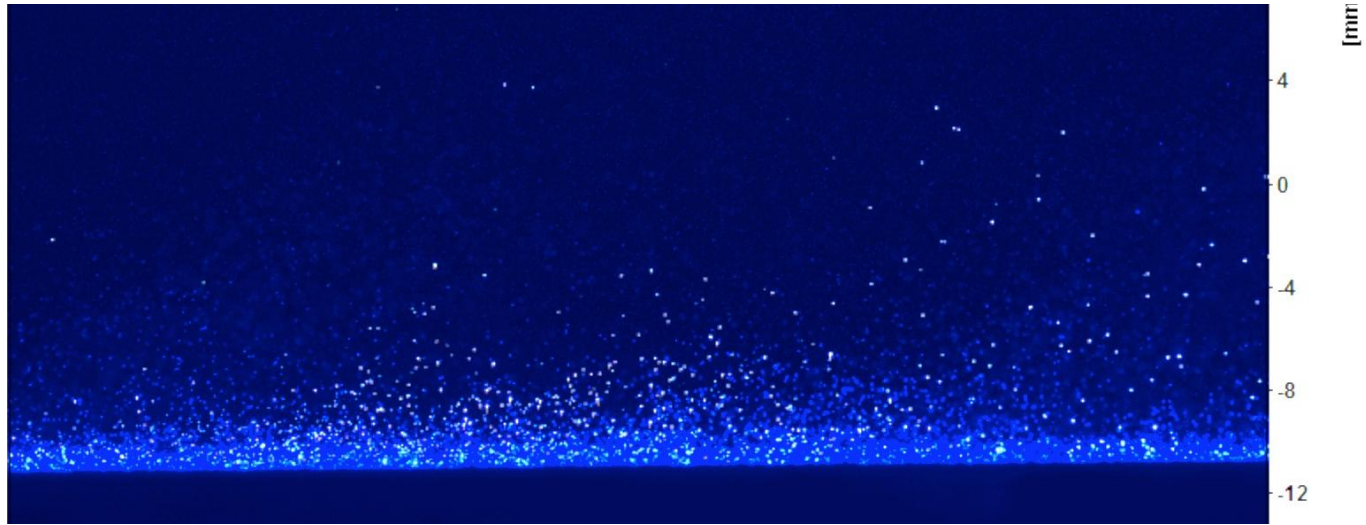
- Repeat with 150 micron...



- More gradual evolution (expected)
- Wavelength similar, but only 1 ripple... decelerating wall jet

# Bed forms important to suspension

Flat bed



Small bedforms

